Tellus (2001), 53A, 1–26
Printed in UK. All rights reserved

Copyright © Munksgaard, 2001
TELLUS
ISSN 0280–6495

Sensitivity of Arctic climate simulations to different boundary-layer parameterizations in a regional climate model

By K. DETHLOFF[1,2]*, C. ABEGG[3], A. RINKE[1], I. HEBESTADT[1] and V. F. ROMANOV[4], [1]*Alfred-Wegener Institute for Polar and Marine Research, Research Department Potsdam, D-14473 Potsdam, Telegrafenberg A43, Germany;* [2]*Institute of Physics, University of Potsdam, D-14415 Potsdam, PF 60 15 53, Germany;* [3]*Deutsche Forschungsanstalt für Luft- und Raumfahrt, D-37073 Göttingen, Bunsenstraße 10, Germany;* [4]*Russian Science Center, The Arctic and Antarctic Research Institute, R-199397 St. Petersburg, Bering Str. 38, Russia*

(Manuscript received 24 March 1999; in final form 3 April 2000)

ABSTRACT

Arctic climate simulations with the high resolution regional climate model HIRHAM show some deviations from station data in the planetary boundary layer (PBL) during winter, which indicates the necessity of improvements in the atmospheric PBL parameterization for a better description of the vertical stratification and atmosphere–surface energy exchange. A 1-dimensional single column model scheme has been used to investigate the influence of two different PBL parameterizations in monthly integrations for January 1991 and July 1990. The first scheme uses the boundary layer parameterization of the atmospheric circulation model ECHAM3, including the Monin–Obukhov similarity theory in the surface layer and a mixing length approach above. The second scheme applies the Rossby-number similarity theory for the whole PBL, connecting external parameters with turbulent fluxes and with universal functions determined on the basis of Arctic data. For both schemes the heat and humidity advection has been determined as residual term of the PBL balance equations. Diabatic sources have been computed from the current model solution and local temperature and humidity changes are estimated from radiosonde data. The simulated vertical structure and the atmosphere–surface energy exchange during January strongly depends on the used PBL parameterization scheme. These different PBL parameterization schemes were then applied for simulations of the Arctic climate in the 3-dimensional regional atmospheric climate model HIRHAM, using ECHAM3 with Monin–Obukhov similarity theory, ECHAM3 with Rossby-number similarity theory and ECHAM4 parameterizations with a turbulent kinetic energy closure. The near surface temperature, the large-scale fields of geopotential and horizontal wind are simulated satisfactorily by all three schemes, but strong regional differences occur. The results show a sensitivity to the type of turbulence exchange scheme used. The comparison with ECMWF analyses and with radiosonde data reveals that during January ECHAM3 with Rossby number similarity theory more succesfully simulates the cold and stable PBL over land surfaces, whereas over the open ocean ECHAM3 with Monin Obukhov similarity works better. ECHAM3 with Rossby-number similarity theory delivers a better adapted vertical heat exchange under stable Arctic conditions and reduces the cold bias at the surface. The monthly mean surface turbulent heat flux distribution strongly depends on the use of different PBL parameterizations and leads to different Arctic climate structures throughout the atmosphere with the strongest changes at the ice edge for January.

* Corresponding author.
e-mail: dethloff@awi-potsdam.de

1. Introduction

The Arctic plays a crucial role in the global climate system, since it is the principal region of radiative energy deficit and atmospheric cooling. Climatic energy equilibrium of the Arctic is maintained by atmospheric energy transports from middle latitudes and by energy influx from the ocean, mainly provided by meso-scale turbulent exchange processes parameterization developed in the atmospheric planetary boundary layer (PBL). An accurate simulation of sea-level pressure and surface winds as well as atmospheric circulation structures in the PBL and in the free troposphere is crucial for a proper simulation of the Arctic climate. Although it is accepted that the Arctic is a region of high climate sensitivity, the understanding of the Arctic climate system determined by radiation processes, atmospheric dynamics, PBL turbulence and the atmosphere–surface energy exchange, is rather poor according to Curry et al. (1996) and Randall et al. (1998).

Bromwich et al. (1994) demonstrated that the typical deficiencies of global climate models for the Arctic region are related to the crudeness of model topography, errors in large-scale dynamics and inadequacies in the physical processes parameterizations. To examine these deficiencies in Arctic climate simulations, Arctic regional climate models have been developed by Walsh et al. (1993), Lynch et al. (1995), Dethloff et al. (1996) and Jürrens (1999). The modelled Arctic climate shows spatial patterns in agreement with observations, but large biases during winter, which are concentrated in the PBL and near the surface. It was suggested that the Arctic climate reproduction should be improved by application of more advanced vertical heat and moisture exchange parameterizations following the ideas of Giorgi et al. (1993) and Brinkop and Roeckner (1995). Giorgi et al. (1993) carried out sensitivity experiments to investigate the influence of PBL parameterization and radiative transfer formulation on climate simulations in the high resolution regional meso-scale model MM4 applied to Europe. Tilley and Lynch (1998) investigated the influences of different land surface schemes and sensible heat fluxes on the Arctic climate as a result of changed surface characteristics. The improvements on account of more advanced radiation and cloud properties have been discussed in Rinke et al. (1997), Pinto and Curry (1997) and Pinto et al. (1999).

The atmospheric PBL provides the physical link between the atmosphere and the earth's surface for exchanges of heat, moisture and momentum. The local energy exchange between the atmosphere and the underlying surface is forced by small-scale turbulence, developing according to the PBL state. It determines the local heat and moisture acquisition from the surface to the atmosphere. The intensity of the small-scale turbulence is affected by large-scale variables like wind, temperature and humidity above the PBL and by surface conditions like roughness, energy influx from the surface and the radiation balance. The PBL parameterization in a climate model is directed to express the small-scale turbulence effects through the large-scale variables, predicted by the climate model and other external parameters as averaged surface roughness and solar radiation. Most of the PBL parameterizations have been developed mainly for middle latitude conditions, where neutral or unstable PBL stratification prevails. However the high latitudes PBL is often characterized by extremely stable vertical stratification. Intensive surface radiative cooling forms vertical temperature inversions and stable stratification especially during polar night condition over land, ice and snow surfaces. Over open water strong heat fluxes from the relatively warm water surface to cold air lead to the development of turbulent convection within the PBL and causes quite unstable stratification. Inhomogenities over the open water surface, drifted sea ice and land determine the horizontal change of surface albedo, roughness parameter and heat flux from the surface. The appearing horizontal changes often can be drastic and similar to frontal zones, leading to quite different heat, moisture and momentum surface-air exchange as discussed in Romanov et al. (1987).

Dethloff et al. (1996) applied the regional climate model HIRHAM, using the physical parameterizations of the Hamburg general circulation model ECHAM3 to simulate the climate of the whole Arctic with a horizontal resolution of 50 km. While the general spatial patterns of surface air temperature, mean sea level pressure and geopotential consist with the European Center for Medium Weather Forecast (ECMWF) analyses, the model shows the largest biases near the surface during winter. The model parameterizations fail to reproduce the strongly stable PBL as a result of intensive surface radiative cooling and lack of solar radiation. To study the influence of different PBL parameterization schemes, first a 1-dimensional version of the HIRHAM model developed by Christensen and Meijgaard (1992), will be used. This 1-dimensional version has been monthly integrated for polar night and polar day conditions to analyse the influence of different parameterization schemes on the development of atmospheric circulation patterns. Integrations were carried out using the original ECHAM3 boundary layer parameterization on the basis of Monin–Obukhov (MO) similarity in the surface layer and a mixing length concept for the remaining PBL. These results are compared with an Arctic PBL parameterization using the Rossby similarity theory developed by Monin and Zilitinkevich (1967) and Blackadar (1967) and adapted to polar conditions by Romanov (1977) and Romanov et al. (1987).

The application of the MO theory is limited to the lowest part of the whole boundary layer, where the turbulent fluxes could be considered as independent from height. The Rossby number similarity theory extends the MO similarity approach to the whole PBL describing also the upper part of the planetary boundary layer. It allows to establish relationships between surface fluxes and their vertical profiles with the flow parameters above the boundary layer and with the surface conditions.

The ability of the model to reproduce the observed flux distribution depends on the parameterization of the PBL and the vertical distribution of these fluxes throughout the boundary layer. The computation and distribution of the fluxes is related to the number of model levels, which is strongly limited in a climate model. In order to study the influence of different PBL parameterizations on atmospheric circulation structures over the Arctic, different versions of the 3-dimensional regional climate model HIRHAM have been investigated. ECHAM3 physics and Monin Obukhov theory, ECHAM3 physics with Rossby number similarity theory and ECHAM4 parameterizations on the basis of turbulent kinetic energy closure have been used for monthly integrations of January 1991 and July 1990 with a horizontal resolution of 50 by 50 km. These integrations are compared with each other and with ECMWF analyses, as well as with radiosonde data for selected stations over the Arctic. The validation against ECMWF analyses is not perfect, since the analyses are model data themselves. Nevertheless this procedure is chosen, because there are only a few observations available from polar regions.

Single column validation of the model against radiosonde data has been a key part of the model development and it provides the insight for isolating relevant mechanisms as pointed out by Randall et al. (1996). The aim of PBL parameterization is to reproduce the sub-grid effects of the local turbulence, which are mainly responsible for the local vertical exchange and the formation of vertical structures. The study of different PBL parameterization schemes in the 1-dimensional version of the HIRHAM model show the idealised influence of the parameterization schemes on the vertical profiles without complicated interactions with other parts of the model. Such an approach allows to concentrate on the PBL scheme without considering deficiences from other parts of the model. After identifying the isolated influence of the different PBL schemes, runs with the full 3-dimensional model HIRHAM with a horizontal resolution of 50 km, including nonlinear interactions among the physical processes have been carried out. Cuxart et al. (1994) proceeded similarly for the investigation of transilient turbulence theory and the exchange coefficient approach and so did Viterbo et al. (1999) for the investigation of the influence of land-surface boundary-layer coupling in the ECMWF model.

In Section 2 the different parameterization schemes will be described. Section 3 contains the 1-dimensional column simulations for January 1991 and July 1990 and presents the influence of different PBL schemes on the 3-dimensional simulations using HIRHAM with a horizontal resolution at 50 km. These model results were compared with radiosonde observations. Finally, Section 4 summarizes the main conclusions.

2. The PBL parameterization schemes

The main aim of the PBL parameterization is to express the small-scale turbulent vertical exchange through large-scale prognostic variables of the climate model. Since the turbulent fluxes and vertical profiles within the PBL depend on various boundary parameters, the common way is to develop relationships between the large-scale variables of the climate model and the sub-grid PBL parameters on the basis of similarity theories using universal dimensionless functions, presented in Abegg (1999).

The 1-dimensional prognostic equations for the mean horizontal wind speed components u, v, potential temperature θ, water vapour mixing ratio q and liquid water content q_l are given by

$$\frac{\partial u}{\partial t} = -\frac{\partial}{\partial z}(\overline{w'u'}) + f(v - v_g), \quad (1)$$

$$\frac{\partial v}{\partial t} = -\frac{\partial}{\partial z}(\overline{w'v'}) + f(u - u_g), \quad (2)$$

$$\frac{\partial \theta}{\partial t} = -\frac{\partial}{\partial z}(\overline{w'\theta'}) + \frac{L_H}{c_p}[(C(\theta) - V(\theta)] + \frac{1}{\rho c_p}\frac{\partial F}{\partial z} - \left.\frac{\partial \theta}{\partial t}\right|_{adv}, \quad (3)$$

$$\frac{\partial q}{\partial t} = -\frac{\partial}{\partial z}(\overline{w'q'}) - C(q) + V(q) - \left.\frac{\partial q}{\partial t}\right|_{adv}, \quad (4)$$

$$\frac{\partial q_l}{\partial t} = -\frac{\partial}{\partial z}(\overline{w'q_l'}) + C(q_l) - P(q_l), \quad (5)$$

where u_g and v_g are the geostrophic wind components, f is the Coriolis parameter, L_H is the latent evaporation heat, c_p is the dry air specific heat capacity for constant pressure, ρ is density and F the net radiation flux. The symbolic terms C, V and P describe the condensation of water vapour, evaporation of rain droplets and the precipitation formation. The last terms in (3) and (4) describe the large-scale contribution to local temperature and humidity time changes, caused by horizontal advection effects. In order to close the system of equations, the turbulent momentum, heat and moisture fluxes, e.g., the first terms on the right hand side of (1)–(5) are expressed through an eddy diffusion assumption. The formulation for the turbulent exchange coefficients of momentum K_m and K_h heat is related to the parameterization concept. The turbulent exchange coefficient for heat is assumed to be equal to the exchange coefficients for humidity and liquid water content.

2.1. *Monin–Obukhov similarity*

The surface layer is defined as the lower part of PBL, where the turbulent fluxes are supposed to be height constant values and the turbulent regime is entirely determined by the three parameters, surface stress $\tau_0 = u_{*0}^2 = [\overline{(u'w')}_0^2 + \overline{(v'w')}_0^2]^{1/2}$, surface heat flux $Q_0 = (\overline{w'\theta'})_0$ and buoyancy parameter $\beta = g/T_0$, with $\overline{(u'w')}_0^2$ and $\overline{(v'w')}_0^2$ as the surface turbulent stress components, u_* the surface friction velocity; $(\overline{w'\theta'})_0$ the kinematic sensible heat flux at the surface, for $z = z_0$ with z as height above the ground and z_0 as roughness length. The gravity acceleration is g and T_0 is a constant mean temperature.

The appearing length-dimension combination is the MO length $L = u_{*0}^2/(\kappa\beta\theta_{*0})$ which describes the typical thickness of the surface layer. $\theta_{*0} = -(\overline{w'\theta'})_0/u_{*0}$ is the turbulent temperature scale. κ is the von Karman constant. The dimensionless combination $\zeta = z/L$ presents a dimensionless height or local stratification parameter. The turbulent fluxes and dimensionless vertical gradients of the mean variables are presented as universal dimensionless functions depending only on the parameter ζ.

$$\frac{\kappa z}{u_{*0}}\frac{\partial u}{\partial z} = \varphi_m(\zeta), \quad (6)$$

$$\frac{\kappa z}{\theta_{*0}}\frac{\partial \theta}{\partial z} = \phi_h(\zeta). \quad (7)$$

Above the surface layer a mixing length approach has been used for the turbulent momentum (index m) and heat (index h) exchange coefficients.

$$K_{m,h} = l_{m,h}^2 \left|\frac{\partial v_h}{\partial z}\right| f_{m,h}(\mathrm{Ri}), \quad (8)$$

where v_h is the horizontal wind speed component and $f_{m,h}(\mathrm{Ri})$ are universal functions of the stability parameter with the Richardson number Ri. To determine the mixing length $l_{m,h}$ the formulation of Blackadar (1962) has been used:

$$1/l_{m,h} = 1/\kappa z + 1/\lambda_{m,h}, \quad (9)$$

where λ_m and λ_h are the asymptotic mixing lengths.

2.2. *Rossby-number similarity*

Above the surface layer within the PBL the Coriolis parameter becomes important for the PBL dynamics. Therefore, Kazansky and Monin (1960) introduced the Coriolis parameter f in the set of governing equations. Thus two length-dimension scales appear, the MO length L and additionally the Kazansky–Monin scale $L_0 = \kappa u_{*0}/f$, presenting the typical PBL thickness scale. Beside the dimensionless height $z_n = z/L_0$, a second dimensionless combination $\mu_0 = L_0/L = -(\kappa^2 \beta Q_0)/(f u_{*0}^2)$ appears, which represents the local stratification parameter.

To express the turbulent PBL fluxes by external variables, predicted in the climate model, the Rossby-number similarity theory for a stationary and horizontally homogeneous PBL has been developed by Monin and Zilitinkevich (1967). It was assumed that the turbulence parameters depend on the external conditions only through the 5 parameters:

G — geostrophic wind speed above the PBL, f — Coriolis parameter, z_0 — surface roughness length, $\Delta\theta = \theta_H - \theta_0$ — potential temperature difference at the top and bottom of the PBL and $\beta = g/T_0$ — buoyancy parameter.

These 5 parameters form two dimensionless combinations. The first is the Rossby number $\mathrm{Ro} = G/(f z_0)$ and the second the integral PBL stratification number $S = \beta\Delta\theta/(fG)$. The PBL turbulent fluxes depend on the external conditions through these 2 dimensionless combinations. Scaling the PBL variables, it is possible to connect internal and external parameters through the universal dimensionless functions η_v, η_α and η_T, depending only on the parameters Ro and S.

$$v_{*0} = G\eta_v(\mathrm{Ro}, S), \tag{10}$$

$$\alpha = \eta_\alpha(\mathrm{Ro}, S), \tag{11}$$

$$\theta_{*0} = \Delta\theta\eta_T(\mathrm{Ro}, S), \tag{12}$$

where α is the angle, presenting the surface wind orientation relative to the geostrophic wind G direction above the PBL.

This formulation also leads to a connection between the local stratification parameter, which includes the surface turbulent heat flux Q_0 and the integral stratification number S, determined by the temperature difference $\Delta\theta$ of PBL top and bottom levels θ_H and θ_0.

$$\mu = \kappa^3 \frac{\theta_{*0}}{\Delta\theta} \frac{G}{v_{*0}} S. \tag{13}$$

According to the similarity theory, vertical profiles of the turbulent exchange coefficients are presented as

$$K_m = K_h = \frac{\kappa^2 u_{*0}^2}{f} K_n(\mu, z_n), \tag{14}$$

where K_n is the dimensionless turbulent viscosity coefficient, performed as universal dimensionless function, depending on the local stratification parameter μ and on the dimensionless height z_n.

$$z_n = (f/\kappa\mu_{*0})z. \tag{15}$$

The ratio of the turbulent heat exchange coefficient to the turbulent viscosity coefficient is usually taken as 1, according to Monin and Yaglom (1971), i.e., $\alpha_T = K_h/K_m = 1$.

Thus, every internal PBL turbulent parameter is defined by boundary conditions only.

2.3. *Parameterization of the boundary conditions*

External parameters included into the numbers Ro and S are related to the PBL top level H, presenting the PBL thickness and depending on the local turbulent regime. Therefore the PBL thickness H is determined by the use of the additional universal dimensionless function γ. According to the similarity concept, the γ-function of the only dimensionless parameter μ is

$$H = \frac{\kappa v_{*0}}{f} \gamma(\mu), \tag{16}$$

where the PBL thickness H is scaled by the Monin–Kazansky scale L_0 and depends on the local PBL stratification.

The external parameter Rossby number Ro includes the wind speed value G at level H and could be extrapolated from the nearest climate model level above H with use of the barotropic presentation or corrected by the thermal wind presence depending on height and on horizontal temperature gradient above the PBL, which is known from the current climate model solution.

The potential temperature values θ_H and θ_0, included into the external parameter S are also principally unknown, because they depend on the local turbulence properties. However, the PBL parameterization (Romanov, 1976a) solves the problem. The topic PBL level H temperature value θ_H is linearly extrapolated from the climate model level z located above H.

$$T_H = T_z + \gamma_a(z - H), \tag{17}$$

where T_z is the temperature at level $z > H$, determined from the climate model and γ_a is the adiabatic temperature vertical gradient for Arctic conditions (Romanov et al., 1987).

The surface heat balance equation is used to close the problem relative to the surface temperature value θ_0.

$$c_p \rho_0 Q_0 + L_H E_0 + q_s + q_m = F, \quad (18)$$

where $L_H E_0$ is the evaporation energy loss, q_s the heat flux from the surface through the quasi-laminar roughness sublayer z_0, q_m is the surface energy loss for ice and snow melting, if θ_0 is above melting temperature and F is the surface radiation balance. Assuming that humidity and temperature profiles are similar in the vicinity of the surface, the turbulent humidity flux is expressed proportionally to the turbulent heat flux, and the evaporation loss $L_H E_0$ is determined through the surface sensible heat flux Q_0. The heat flux from the surface is determined from the ECHAM3 parameterizations, using the calculated surface air temperature θ_0. The universal dimensionless functions for η_v, η_α and K_n used for the parameterizations are determined as a multilevel nonlinear differential numerical automodel solution of the PBL (Romanov, 1976b). They are verified by Arctic data and defined in form of graphs in (Romanov, 1977, Romanov et al., 1987, see also the appendix of Abegg, 1999).

The differential kinetic energy balance equation and Kolmogorov hypothesis, which connects the turbulent viscosity coefficient and kinetic turbulent energy with the mixing length, are used to close the problem as well as the von Karman hypothesis, generalized for the stratified PBL. The sensible turbulent heat flux is described by the differential heat balance equation.

3. Influence of different PBL parameterizations on atmospheric structures

The model employed in this study is the regional atmospheric climate model HIRHAM, developed by Christensen et al. (1996), which has been applied to the Arctic Basin by Dethloff et al. (1996) and Rinke et al. (1997, 1999). HIRHAM uses either the physical parameterization of the ECHAM3 general circulation model, (Roeckner et al., 1992) or of the ECHAM4 general circulation model (Roeckner et al., 1996).

HIRHAM is a hydrostatic primitive equation regional atmospheric model based on the adiabatic formulation of the HIRLAM system (Machenhauer, 1988; Gustafsson, 1993) and the physical parameterizations of the global model ECHAM. The horizontal grid uses rotated latitude/longitude coordinates with north pole at 0°N and 0°E, a resolution of 0.5° by 0.5°. The lateral boundary scheme is the simplified Davies (1976) relaxation over 10 grid points. The semi-implicit leapfrog time-stepping scheme with Asselin time filtering has been used.

The radiation scheme in ECHAM3 is based on Hense et al. (1982). The ECHAM4 radiation scheme is in accordance with Morcrette (1989) and takes into account improved parameterization of the water vapour continuum (Giorgetta and Wild, 1995). Both model versions use stratiform clouds (Sundqvist, 1978, Roeckner et al., 1991), cumulus convection (Tiedtke, 1989; Nordeng, 1994) and gravity wave drag formulation (Palmer et al., 1986; Miller et al., 1989).

A land-surface parameterization package has been applied which comprises a 5-layer soil with predicted temperature, a bucket model for the soil water, vegetation effects and a run-off scheme (Dümenil and Todini, 1992) with soil characteristic fields from Claussen et al. (1994) and Roeckner et al. (1996).

A simple sea-ice treatment is based on the sea surface temperature (SST), assuming sea ice when the SST is below 271.37 K and calculating the skin temperature according to a linearized heat balance equation. A fixed sea ice thickness of 2 m is used. The SST is taken from ECMWF analyses, updated daily.

The ECHAM3 PBL scheme uses the Monin Obukhov similarity theory in the surface layer with the universal dimensionless functions of Louis (1979) and a mixing length approach following Blackadar (1962) above the surface layer, described in DKRZ (1992). In ECHAM4 a PBL scheme according to Brinkop and Roeckner (1995) and Roeckner et al. (1996) has been used, which bases on an additional turbulent kinetic energy equation with an exchange coefficient approach.

In this study simulations with HIRHAM including the original physical parameterizations of ECHAM3 and ECHAM4 habe been carried out.

Additional runs were performed in which the PBL turbulence closure scheme of ECHAM3 was replaced by the Rossby-number similarity theory, updated for the Arctic. In a first step single-column versions of each model have been used in order to test the different turbulence closure schemes. Simulations with ECHAM3 physics and Monin Obukhov similarity theory in the surface layer and the Rossby-number theory approach for the whole PBL parameterization are compared. In a second step the influence of different PBL parameterization schemes on the Arctic atmospheric circulation was studied with the corresponding 3-d versions of HIRHAM. These simulations were compared with radiosonde data for individual station points. In order to distinguish the simulation runs of the regional atmospheric climate model HIRHAM with three different PBL parameterizations the following abbreviations have been used:

ECHAM3_MO — ECHAM3 with Monin Obukhov mixing length parameterization,

ECHAM3_RO — ECHAM3 with Rossby number similarity parameterization,

ECHAM4 — ECHAM4 with turbulent kinetic energy closure.

3.1. *Simulations with the 1-dimensional column model*

Betts and Miller (1986), Cuxart et al. (1994) and Randal et al. (1996) developed the idea of applying single column models to test parameterizations under development for general circulation models. In this approach a parameterization is exercised in the framework of a single atmospheric column, which can be thought of as a single atmospheric column taken from a global climate model. The tendencies of temperature and moisture due to horizontal advection are used to force the single column model. Objective analysis methods from various sources like radiosondes and wind profilers can be used to obtain synoptic descriptions of the large-scale forcing fields. Alternatively, data assimilation products of numerical weather prediction centers can be used. In the latter case the problem of affecting the forecast results of the model by the applied physical parameterizations arises, which is particularly important in data-sparse regions like the Arctic. Randall and Cripe (1999) discussed the advantages and disadvantages of the different possibilities for prescribing advective tendencies and pointed out that among the different methods of specifying the observed forcing for 1-dimensional column models each method has its own strengths and weaknesses.

In our approach we apply the single column version of the HIRHAM model as a test tool to identify the qualitative influences of different PBL parameterizations. Therefore we used a procedure of determining the advective forcing within the limits of acceptable simplicity. The simulation results of a 3-dimensional climate model are complicated and depend on all aspects of that model, so that it can be very difficult to attribute qualitative deficiences of the results to special aspects of the model parameterizations. Single column version runs allow to test parameterizations without complications from the rest of a climate model. The vertical feedbacks inside the single column version are active, whereas those involving the large-scale circulation cannot be included. The PBL scheme could for instance have an impact on cloud cover and radiation. Consequently, the full nonlinear interaction between the vertical and the horizontal feedbacks can be studied only with the 3-dimensional model.

The 1-dimensional version (1d) of the regional climate model HIRHAM was developed by Christensen and Meijgaard (1992). This model contains all physical parameterizations of ECHAM3, including radiation, clouds, convection, land-surface processes, gravity wave drag and PBL processes (Roeckner et al., 1992). The original 1d model does not include any horizontal heat and moisture advection, although this advection presents an important process to compensate the local energy loss caused by diabatic cooling, as typical for Arctic winter conditions. In order to integrate a 1d model over a time period of one month, it is necessary to include horizontal advection. Therefore in this study local energy sources or sinks owing to horizontal advection have been taken into account, acting in the conservation equations for heat (3) and humidity (4), described in Section 2.

Local temporal temperature and humidity changes might be caused not only by horizontal advection, but also by the total effects of the local diabatic processes at the same point. Assuming that the 1d model simulates the local diabatic processes realistically, the advection effects can be determined by substracting the local temporal changes provided from radiosonde data from the total diabatic sources computed by the current model. That means, the horizontal advection is determined as residual term to satisfy the heat and humidity balance equations:

$$\left.\frac{\partial\theta}{\partial t}\right|_{\mathrm{Adv}} = \frac{\partial\theta}{\partial t} - \left.\frac{\Delta\theta}{\Delta t}\right|_{\mathrm{Data}}, \tag{19}$$

$$\left.\frac{\partial q}{\partial t}\right|_{\mathrm{Adv}} = \frac{\partial q}{\partial t} - \left.\frac{\Delta q}{\Delta t}\right|_{\mathrm{Data}}. \tag{20}$$

The 1d model was integrated in time, initialized with the temperature, humidity and wind radiosonde profiles. Advective forcing terms for the heat and humidity balance equations have been determined from radiosonde data. The horizontal momentum advection is assumed to be negligible. A vertical 25 levels resolution is used, whereby the lowest 8 levels are in the PBL. The time step for all integrations is 300 s. The calculations described here for January 1991 and July 1990 were performed at the Arctic land point Norman Wells (65.3°N, 126.8°W).

The described approach of calculating the advection terms forces the model to match the radiosonde observations for single station points. First the advective tendencies has been computed on the basis of ECHAM3_MO. The same advective tendencies have been applied to the experiments using ECHAM3_RO. Figs. 1a, b show the comparison of the temperature simulated by using ECHAM3_MO with radiosonde data for January and July conditions at the Arctic land point Norman Wells. As is evident from the height–time cross-sections, the simulated temperature is well-following the data in the whole atmosphere mainly as a result of the prescribed advective forcing. Accordingly, the monthly averaged temperature profile agrees well with observations. Deviations between model simulations and station data are in the range of natural interannual variability. No attempt was made to calibrate the parameterization schemes to produce the best possible simulations. The 1-dimensional validation reveals that the vertical temperature and humidity profiles are realistic if the correct forcing is imposed.

Figs. 2a, b present the monthly mean vertical profiles of sensible heat flux, computed in the 1d model with the same prescribed advection terms using ECHAM3_MO and ECHAM3_RO for January and July conditions, respectively. Largest flux differences as a result of different PBL parameterizations occur during January at the lowest model levels. ECHAM3_MO model results show nearly neutral stratification, if the sensible heat flux values are close to zero within the surface layer and up to the PBL top. On the contrary by using ECHAM3_RO pronounced negative heat fluxes were produced over the whole PBL depth with maximum values of about $-15\ \mathrm{W/m^2}$. The greatest differences occur in the lowest model levels for January. The monthly mean temperature differences reach 4 to 6°C, and humidity differences exceed 0.5 g/kg near the surface, not shown here. The comparison of these two different parameterizations also shows, that the PBL height is reduced for January conditions, when Rossby number similarity is used for the parameterization of the PBL. Both parameterizations produce quite similar profiles above 1500 m. The Rossby number similarity scheme results in a more stable stratification than the MO-mixing length scheme. Similar calculations have been carried out during January for the Russian land point Norilsk (69.3°N, 88.3°O), not shown here. These computations confirm the result that the Rossby number similarity scheme leads to a more stable stratification than the MO-mixing length scheme. Whereas for ECHAM3_MO the thermal stratification is neutral or slightly unstable, for the ECHAM3_RO runs pronounced time intervalls with stable conditions occur. Significant differences between the time evolution of the models are connected with periods of stable conditions. For July the vertical sensible heat flux profiles are quite similar for both parameterizations.

The main focus of the experiments with the 1d version of HIRHAM under the influence of a simple but realistic advective forcing was the determination of the influence of different turbulence parameterizations on simulated Arctic temperature and humidity profiles for mean winter and summer conditions. Serreze et al. (1992) discussed the existence of Arctic temperature inversion near the surface. This temperature inversion has been reproduced in our 1d dimensional simulations. Since the physical control of Arctic inversions is a complex phenomenon, which involves not only radiative cooling, but also warm-air advection, subsidence, surface melt and topographic influ-

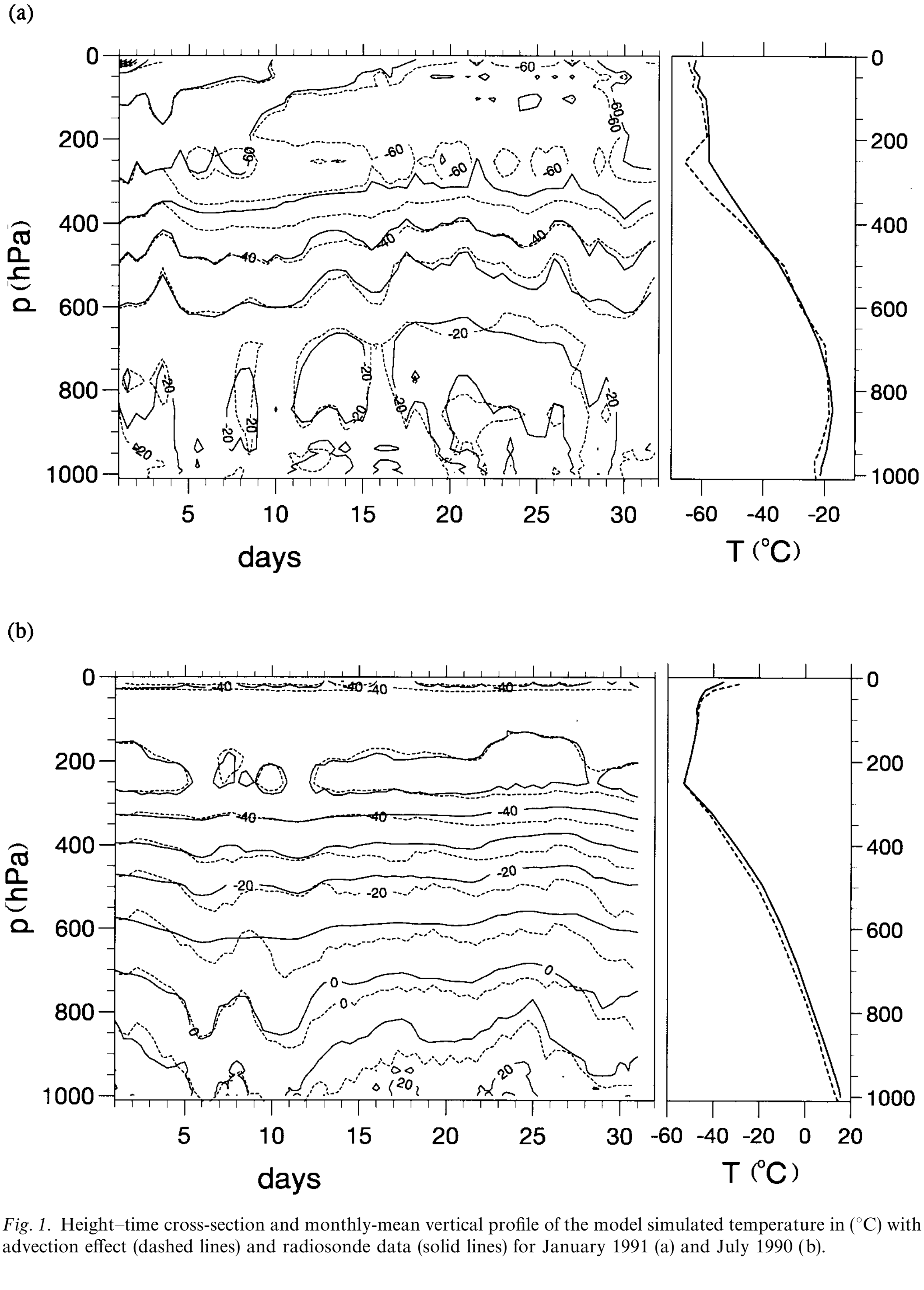

Fig. 1. Height–time cross-section and monthly-mean vertical profile of the model simulated temperature in (°C) with advection effect (dashed lines) and radiosonde data (solid lines) for January 1991 (a) and July 1990 (b).

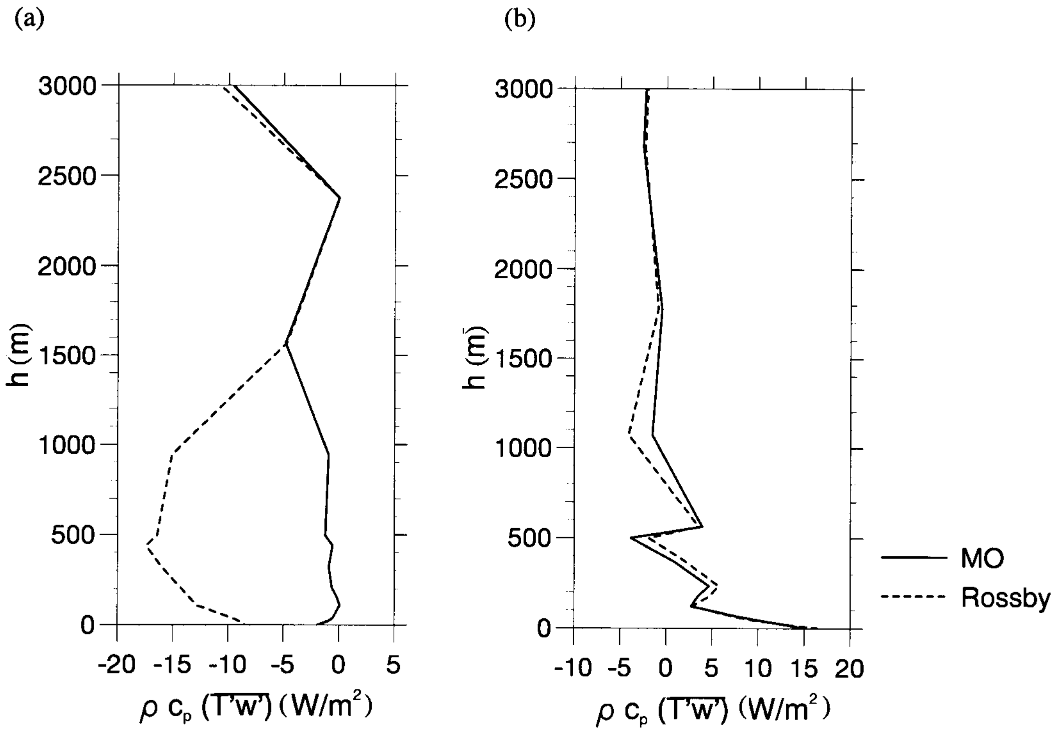

Fig. 2. Monthly averaged vertical profiles of the sensible turbulent heat flux in (W/m^2), simulated by ECHAM3 version with MO-mixing length similarity (solid lines) and ECHAM3 version with Rossby-number similarity (dashed lines) for January 1991 (a) and July 1990 (b).

ences, a better understanding requires full interactions in the 3d simulations, as described in the following.

3.2. *Simulations with the 3-dimensional regional climate model*

The influence of different PBL parameterization schemes on the atmospheric circulation structures over the Arctic has been studied in the 3-dimensional regional climate model HIRHAM with a horizontal resolution of 0.5°. In the following the simulation results using three fundamentally different PBL parameterizations (ECHAM3 with MO mixing length parameterization, ECHAM3 with Rossby number similarity parameterization and ECHAM4 with TKE closure) are discussed. These simulations were compared with local vertical temperature profiles for individual station points on the basis of radiosonde data.

3.2.1. Near surface temperature and surface sensible heat fluxes. The near surface temperature is a useful variable to determine the quality of a regional climate model. The comparison of the simulated near surface temperatures for January 1991 with those obtained from the ECMWF analyses is shown in Fig. 3. The spatial distribution of the simulated near surface temperature is in agreement with the ECMWF analyses. The main features as the high temperatures over the North Atlantic as well as the low temperatures over the Arctic Ocean are well simulated with all 3 PBL schemes. The differences over continental areas are in the range of ca. 5°C. The different schemes used in the regional model seem to overestimate the temperatures in large areas of the integration area, especially over continental areas. In view of the results of Viterbo et al. (1999) these differences are probably connected with missing parameterizations of frozen soil and permafrost processes.

The simulated near surface temperatures for

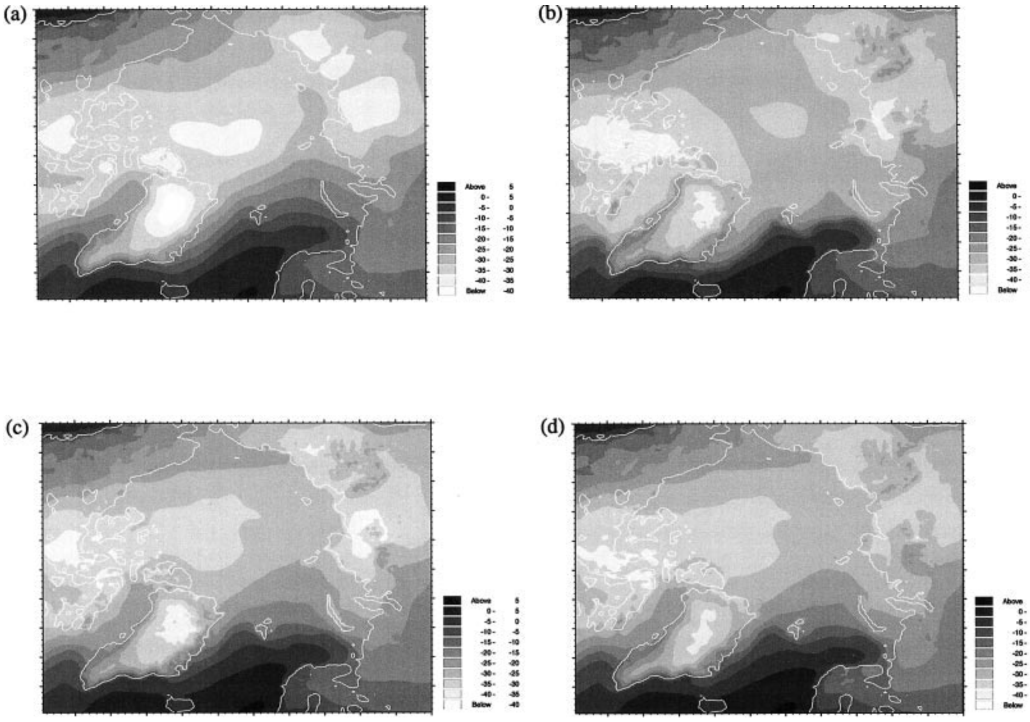

Fig. 3. Monthly mean near surface air temperature in (°C) for January 1991, from (a) ECMWF analyses, (b) simulated by ECHAM4 version, (c) simulated by ECHAM3_MO scheme, (d) simulated by ECHAM3_RO scheme.

July 1990 are shown in Fig. 4. The spatial distribution of the near surface temperature is in satisfactory agreement with the ECMWF analyses. The indicated differences over Greenland, the Arctic Ocean and the continental areas result from the application of different PBL schemes.

Figs. 5a and Fig. 6a display the monthly mean surface sensible heat fluxes over the Arctic for January 1991 and for July 1990, respectively, obtained by using ECHAM3_MO. During summer the energy flux into the atmosphere over land reaches values of 50 to 70 W/m^2 and almost everywhere over the ocean and ice surfaces neutral or slightly stable stratification prevails. During winter land and ice areas show mostly negative surface heat fluxes indicating downward fluxes from the atmosphere to the surface. A pronounced stable stratification occurs in areas over the central Arctic, Greenland, the Northern Canada territories and continental areas of Northern Europe and Asia, where the surface sensible heat flux reaches negative values around -30 W/m^2. Positive energy flux from the surface into the atmosphere takes place mostly over the ocean surface, where the water surface temperature is much higher than the air surface temperature. The strongest positive heat flux of 50 to 60 W/m^2 occurs over the ice-free-water areas near the ice edge, because colder air moves from the ice covered surface to the warm ice-free water surface, which leads to the occurrence of unstable stratification.

Our results are in agreement with the investigations of Overland et al. (1997), who determined sensible heat fluxes for a 5 year climatology on the basis of the Goddard general circulation model GEOS-1, taking into account observational data from conventional sources plus aircrafts, ships, radiosondes, satellite retrieval and cloud motion winds.

Figs. 5b, c show the differences of the surface sensible heat flux distributions between model runs due to different boundary layer parameterizations for January 1991 and Figs. 6b, c for July 1990. The ECHAM4 version generates a more stable PBL stratification during January in a narrow belt to the north of the ice edge, where

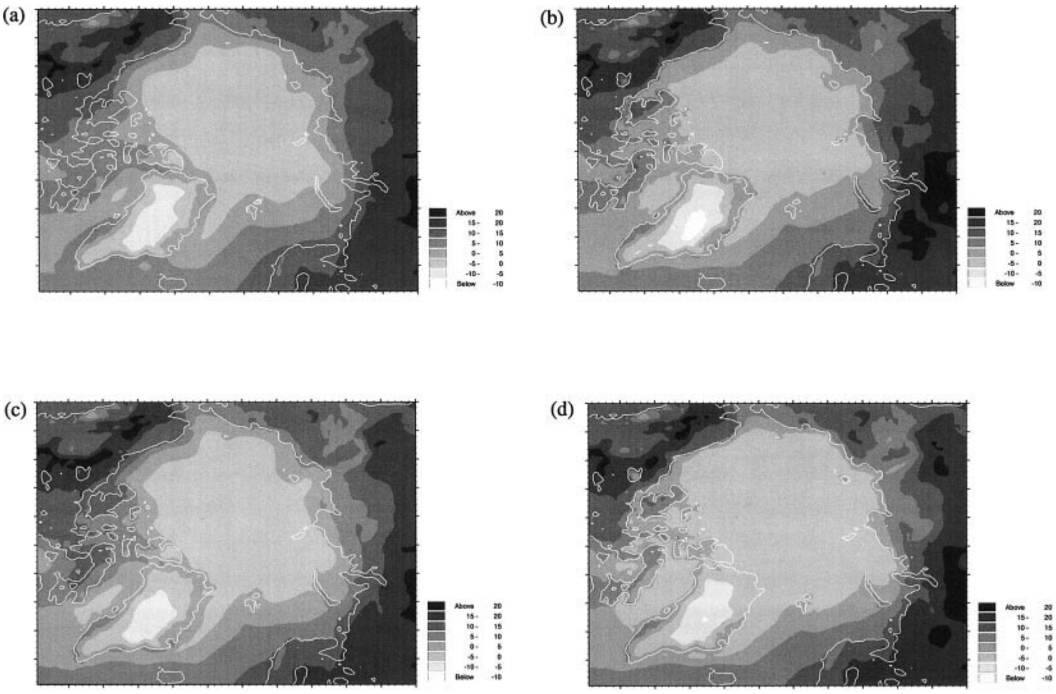

Fig. 4. Monthly mean near surface air temperature in (°C) for July 1990, from (a) ECMWF analyses, (b) simulated by ECHAM4 version, (c) simulated by ECHAM3_MO scheme, (d) simulated by ECHAM3_RO scheme.

negative fluxes appear and a more unstable PBL stratification develops south of the ice edge over open water. A similar picture is produced by ECHAM3_RO for January in Fig. 5c but with a more stable stratification over Greenland and other continental land areas. The most pronounced changes compared to ECHAM3_MO appear over the continental areas of Greenland, Northern America and Asia.. In all runs the north ice edge zone is influenced by relatively warm air coming from the open water areas which forms intensive downward heat fluxes to the cold ice and snow surface during winter. This northward flow of relatively warm air is most strong in the case of ECHAM3_RO, presented in Fig. 7d. The discrepancies with the observations of Overland et al. (1997) are in the same range as those between the models and it is impossible to judge the different PBL schemes on the basis of the available observations.

In Fig. 6b the ECHAM4 run for July produces stronger positive surface heat fluxes from the surface into the atmosphere mostly over continental land areas. In Fig. 6c the surface heat fluxes distribution for July, determined by the ECHAM3_RO run reveals the greatest changes over land points. Limited areas along the coastal line can be found, where the strong temperature contrast between land and ocean induces an unstable PBL as a result of higher positive surface heat fluxes as in the ECHAM3_MO version. It appears that the near surface flow, simulated with Rossby-number similarity theory is more stable almost everywhere over the ice-covered Arctic Ocean compared to the ECHAM3 version with MO theory. The most intensive downward directed heat flux covers a limited belt to the north of the coastal line, where a relatively cold water surface takes up quite a lot of atmospheric energy for summer heating. Only a narrow zone to the south of the Norther American coastal line is characterized by more unstable stratification, produced by the ECHAM3 version with the MO similarity. The surface heat flux differences over this zone reach 30 to 40 W/m^2.

Different PBL parameterizations may produce

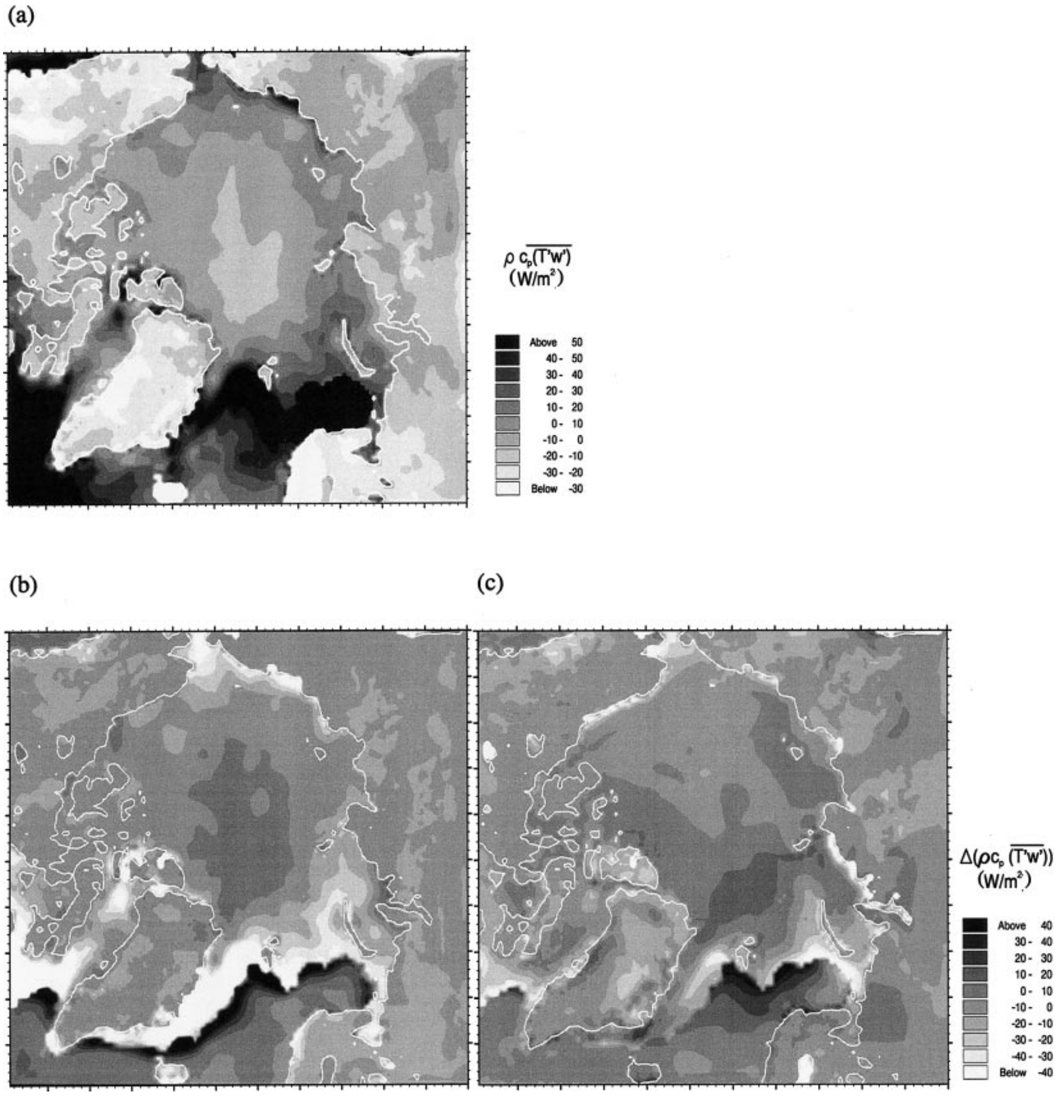

Fig. 5. (a) Monthly mean surface sensible heat flux in (W/m^2) for January 1991, (a) simulated by the ECHAM3 version with MO-mixing length PBL parameterization, (b) differences "ECHAM4 minus ECHAM3_MO version", (c) "ECHAM3_RO minus ECHAM3_MO version".

significant differences in the monthly climate distributions of energy exchange between the atmosphere and the surface over high latitudes, where generally an intensive energy exchange exists. The largest changes in the sensible heat fluxes occur at the oceanic sea-ice border between the Greenland sea and the southern part of Spitsbergen during winter, influencing especially the temperature distribution in this area. During summer the differences on the sea-ice border are not pronounced. One consequence of the low temperatures during winter, which leads to the development of a very stable Arctic PBL owing to the high longwave emissivity of snow and ice surfaces and the missing incoming short wave radiation is a continuous cooling on the surface in the Arctic. In agreement with the 1d model the 3d simulations clearly show a stronger stability

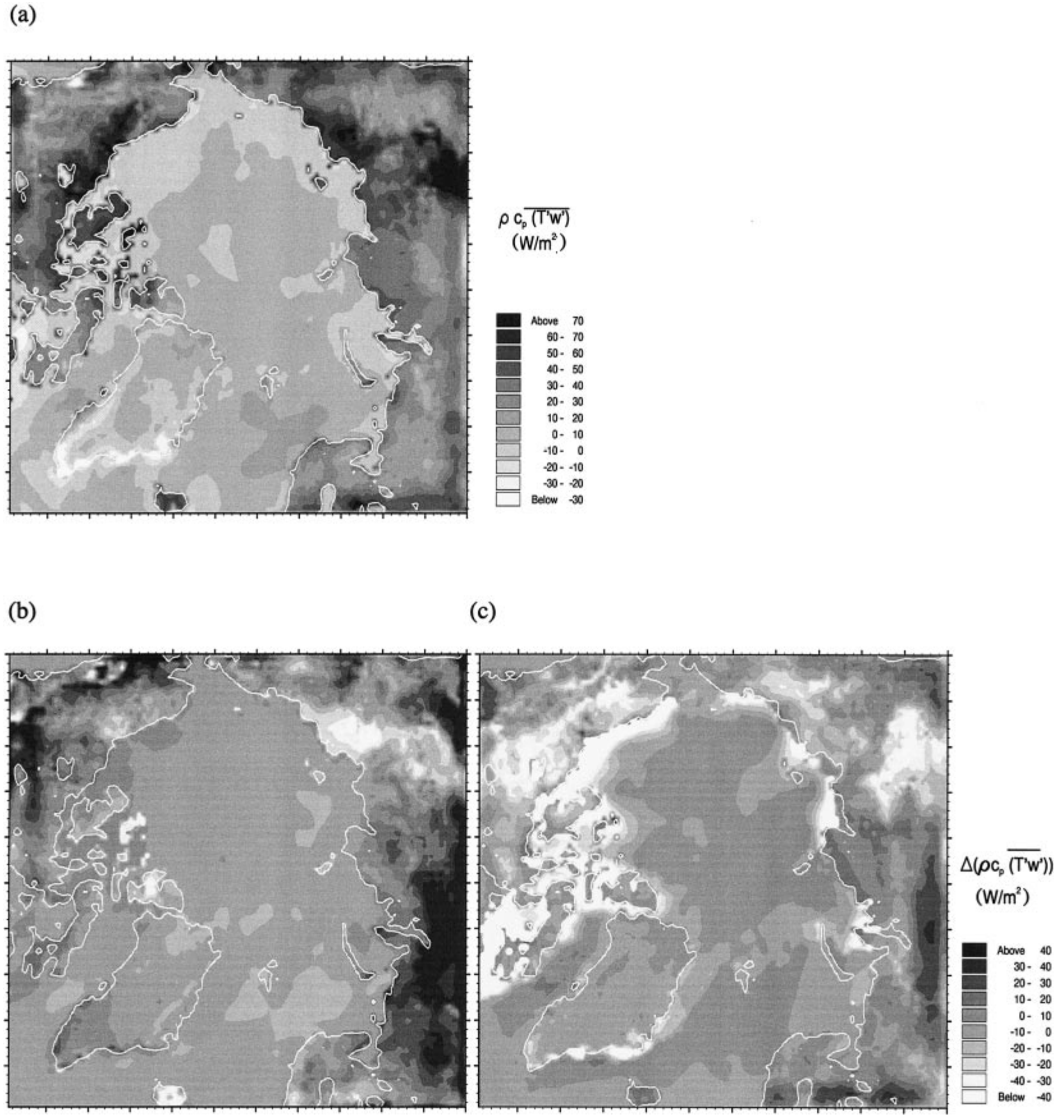

Fig. 6. (a) Monthly mean surface sensible heat flux in (W/m^2) for July 1990, simulated by the ECHAM3 version with MO-mixing length PBL parameterization, (b) differences "ECHAM4 minus ECHAM3_MO version", (c) "ECHAM3_RO minus ECHAM3_MO version".

for the ECHAM3_RO PBL scheme over land and sea-ice points.

Handorf et al. (1999) revealed the existence of moderately to extremely stable stratification and the existence of shallow boundary layers beneath these stability conditions. Derbyshire (1995) characterised terrain-generated effects, meso-scale influences, gravity waves, variations in synoptic flow and cloud cover variations as the main sources of variability in stable boundary layers. The identification and contribution of these different nonlinear physical processes, all contained in the employed regional atmospheric climate model HIRHAM were beyond the scope of this work and would need further research. To which extent the variability of stable boundary layers is controlled by external orographic effects and other spontaneous causes due to synoptic flow instabilities is not yet understood and has to be investigated further.

3.2.2. Large-scale geopotential and wind structures. Figs. 7a–d show the geopotential height and wind distributions above the PBL over the whole Arctic at the 850 hPa level for January 1991 on the basis of ECMWF analyses, the ECHAM4 version, the ECHAM3_MO and the ECHAM3_RO turbulence scheme. The Figs. display the transport over the central Arctic, directed from Siberia to Norther America. There exist lows, which are centred over

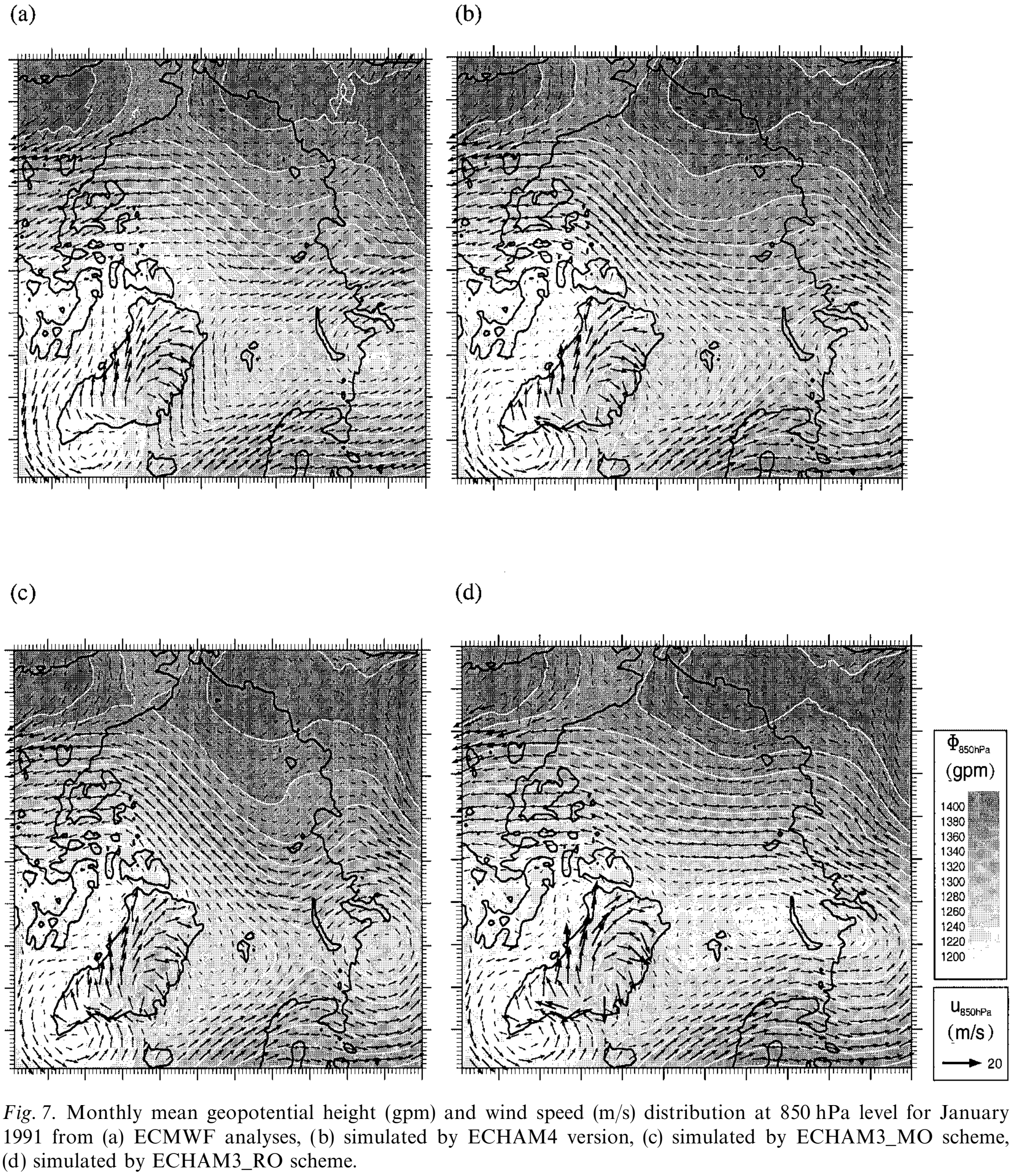

Fig. 7. Monthly mean geopotential height (gpm) and wind speed (m/s) distribution at 850 hPa level for January 1991 from (a) ECMWF analyses, (b) simulated by ECHAM4 version, (c) simulated by ECHAM3_MO scheme, (d) simulated by ECHAM3_RO scheme.

the Labrador Sea and over the Kara Sea as well as a pressure depression over Spitsbergen. High pressure structures occur over Siberia and Alaska. Comparing the structures of the ECMWF analyses in Fig. 7a with the ECHAM3_MO simulations in Fig. 7c, the ECHAM3_MO run generates a more pronounced flow over the central Arctic. Fig. 7a shows prevailing southward directed winds in the Fram Strait. These winds are weakened and entirely substituted by northward directed winds using the ECHAM4 and ECHAM3_MO simulations.

Overall the ECHAM3_RO run gives the best agreement with the ECMWF analyses. Assuming the ECMWF analyses as a validation tool, the southward transport through the Fram Strait indicated in the ECMWF analyses is visible only in the simulations with the ECHAM3_RO PBL scheme. This strongly supports the assumption that this scheme more realistically simulates cold out breaks from Greenland to the south and that it reasonable works in the case of a stable PBL with strong winds. Because of the influence of the wind fields on the drift of sea ice the use of the best appropriated PBL scheme is strongly required in coupled atmosphere-ice-ocean models as discussed in Jürrens (1999).

Overland et al. (1997) stated that regional differences in the atmospheric thermal energy budget are related to the tropospheric circulation pattern in the Arctic. The consistent spatial near surface temperature pattern with coldest temperatures in the western Arctic north of Canada and warmer regions in the Chukchi, Greenland, and the Barents Seas are simulated (compare Figs. 3b–d) and connected with the tropospheric geopotential fields. The Figs. 7a–d exhibit strong katabatic wind fields over Greenland, the strong Islandic low and a persistent low located over Northern Canada. The cyclonic flow around the low is the tropospheric extension of the strong polar vortex with the centre over the Arctic Ocean in 500 hPa, not shown here. This vortex also steers mid-latitude transient weather systems which transports heat from the Atlanic Ocean into the eastern Arctic, increasing the temperatures in the Barent Sea and on its return causing the deep temperatures over Northern Canada. The differences in the position of the polar vortex at 500 hPa as a result of different PBL schemes are quite considerable.

Figs. 8a–d present the geopotential height and wind speed distributions over the whole Arctic at the 850 hPa level for July 1990 on the basis of ECMWF analyses, ECHAM4, ECHAM3_MO and ECHAM3_RO. The ECMWF analyses in Fig. 8a show a cyclone over the central Arctic and an anticyclone over Greenland. Whereas the ECMWF analyses points out prevailing winds over the East Siberian Sea, blowing from East to West and turning to the South over Siberian territories, the ECHAM3_MO formulation in Fig. 8c generates the opposite flow from West to East. The ECHAM4 version in Fig. 8b simulates a low over the central Arctic, which extends more to the Siberian territories. The low over Siberia which appeared in the ECMWF analyses, disappears and the high over Greenland seems more developed. The monthly mean circulation structures produced by ECHAM3_RO in Fig. 8d are characterized by a deeper low over the Central Arctic.

The large-scale fields of geopotential and wind are simulated satisfactorily by all three schemes, but strong regional differences occur. The best agreement with the ECMWF analyses during summer has been obtained with the ECHAM4 scheme using a TKE closure. For all PBL schemes the lowest temperatures occur over the Arctic Ocean. These temperatures are higher in July than during January as a result of incoming solar radiation and of transient weather systems, transporting more heat into the Central Arctic.

3.2.3. Temperature bias and temperature profiles at selected grid points. The temperature bias of the different PBL schemes compared to the ECMWF analyses was computed for January 1991 and July 1990 as spatial mean for all grid points in the whole integration area excluding the 10 grid points width boundary zone. The averaged results for all land points, all points covered by sea-ice and all ocean points are presented in Fig. 9 for January 1991 and in Fig. 10 for July 1990. In both months the largest deviations of about 3–4°C occur over sea-ice points. Over land points the deviations are within the range of 2–3°C, whereas they are rather small over ocean points. The temperature bias is connected with a similarly strong bias in the specific humidity of about 0.15 g/kg and great changes in the cloud structures, not shown here. The best agreement with the ECMWF humidity

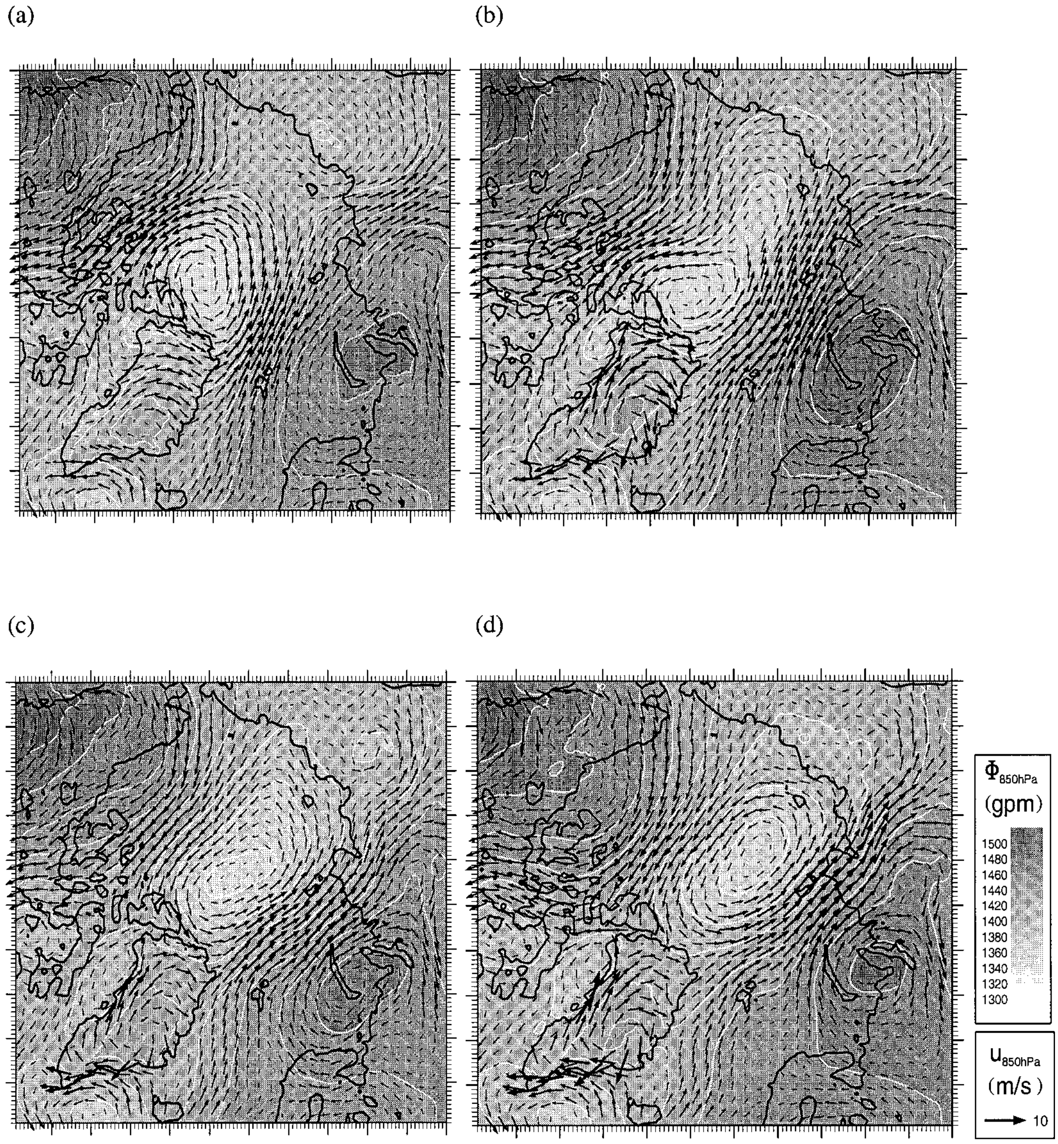

Fig. 8. Monthly mean geopotential height (gpm) and wind speed (m/s) distribution at 850 hPa level for July 1990 from (a) ECMWF analyses, (b) simulated by ECHAM4 version, (c) simulated by ECHAM3_MO scheme, (d) simulated by ECHAM3_RO scheme.

analyses during winter has been obtained with the ECHAM3_RO version, not shown here.

Over land and sea-ice points the temperature profile shows a surface inversion as a result of cooling due to outgoing long-wave radiation. The temperature maximuma at about 920 hPa are caused by heat inflow connected with synoptic weather systems. Serezze et al. (1992) analysed the occurrence of low-level Arctic temperature inversions using 12 years of temperature sounding data from 31 Eurasian coastal, inland, and Soviet drifting stations. These analyses revealed that inversions tend to be more intensive during winter due to a large deficit in surface net radiation. Overland

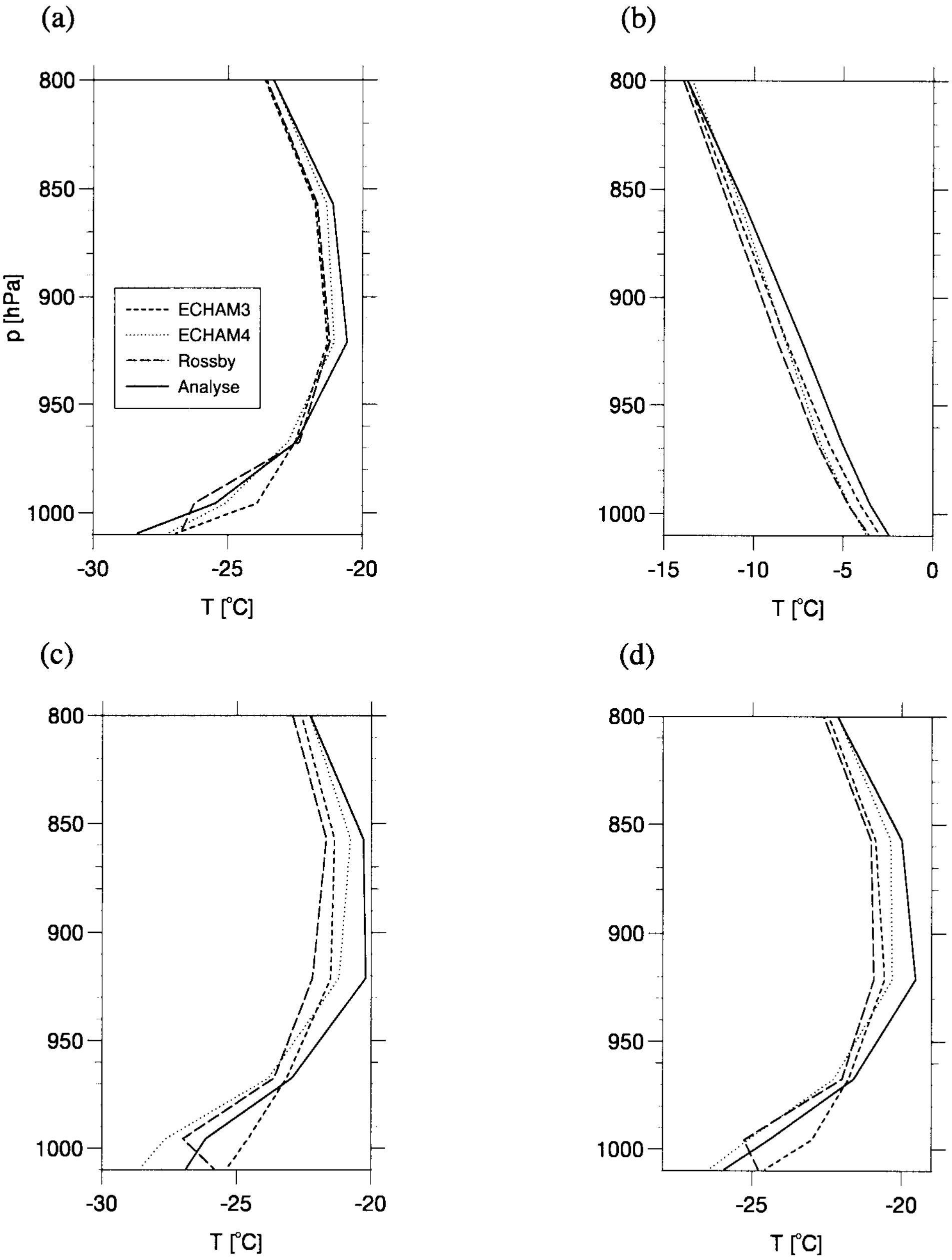

Fig. 9. Monthly averaged temperature profiles in (°C) for January 1991 as mean over all land points (a), all ocean points (b), all sea-ice points (c) and all integration points (d), simulated by ECMWF, ECHAM4 version, ECHAM3_MO scheme, ECHAM3_RO scheme.

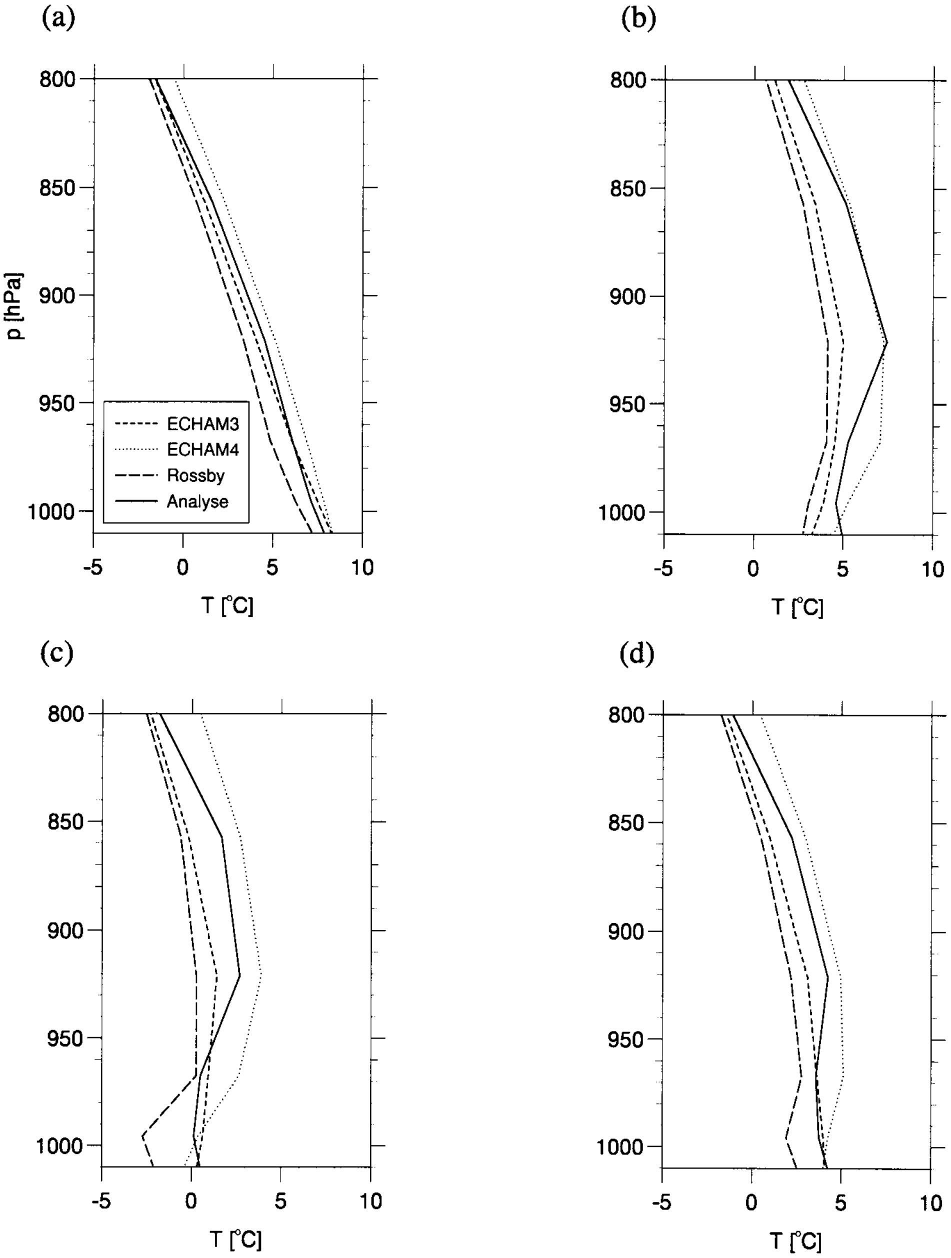

Fig. 10. Monthly averaged temperature profiles in (°C) for July 1990 as mean over all land points (a), all ocean points (b) , all sea-ice points (c) and all integration points (d), simulated by ECMWF, ECHAM4 version, ECHAM3_MO scheme, ECHAM3_RO scheme.

and Guest (1991) showed that during winter, when solar radiation is absent, variations in cloud cover have a marked effect on the radiation budget, surface temperatures and hence the inversion layer. The different PBL schemes show pronounced differences in the vertical humidity and hence the cloud profiles.

The decoupling of the surface fluxes from fluxes in the atmospheric PBL was investigated by Derbyshire (1999). He proposed a positive feedback between turbulence of the stable stratified PBL and surface temperature as a result of decoupling. In the ECHAM3_RO PBL scheme there are no hints on a positive feedback, since the reduced turbulence in more stable conditions is not connected with lowered surface temperatures. On the contrary because of the reduced turbulence the surface temperature increases, indicating a negative feedback process. Since the surface flux does not only depend on the temperature profile but also on the wind profile, which is also strongly affected by stability, the nonlinear problem is so complex that this behaviour is not comprehensively understood. As suggested by Derbyshire (1999), more idealized modelling on this topic is needed. McNider et al. (1995) pointed out, that if thermal stability dominates over the wind shear, the generation of turbulent kinetic energy is suppressed and the surface become decoupled from the layers above. This leads to weak winds on the surface while the vertical transfer of momentum is reduced. Furthermore, the surface cools rapidly due to the interrupted heat transfer from above. This situation can produce extremely low surface temperatures. On the other hand, if the wind shear develops faster than the thermal stability, high levels of turbulence can be supported by production of turbulent kinetic energy. This maintains momentum and heat fluxes from above, leading to warmer and windier conditions near the surface. On the basis of investigations with the ECMWF model Viterbo et al. (1999) estimated a severe cold bias over continental ares in winter. This was caused by a positive feedback, inherent in the stable boundary layer scheme, similar to our ECHAM3_MO scheme, that amplifies a near-surface cold bias. If the surface becomes too cold, the boundary layer becomes more stable, further reducing the downward heat flux, which results in even more cooling on the surface. Viterbo et al. (1999) suggest that this positive feedback is more pronounced in the ECMWF model than in the real atmosphere. Therefore, an improved parameterization has been applied with increasing heat diffusion during stable conditions by use of revised stability functions. Our ECHAM3_RO scheme with Rossby number similarity and universal functions developed for Arctic conditions by Romanov et al. (1987) seems to avoid such cold bias on the surface and delivers a better adapted vertical heat exchange under stable Arctic conditions.

Monthly mean vertical temperature profiles at selected grid points for January 1991, calculated from integrations of model runs with ECHAM3_MO, ECHAM4 and ECHAM3_RO were compared with radiosonde data. Fig. 11 shows the mean sea level pressure for January 1991 with the Siberian High (SH), the low over the Russian Arctic (RA) and European Arctic (EA), the Islandic Low (IL), the pressure ridge over the Arctic Ocean (AO) and the Alaskian High (AH). For each of these main pressure centres two individual stations were selected in order to compare the model results with observations.

Fig. 12 depicts the differences of the monthly averaged temperature profiles between model simulations and radiosonde observations for the 6 main areas SH, RA, EA, IL, AO, AH. The

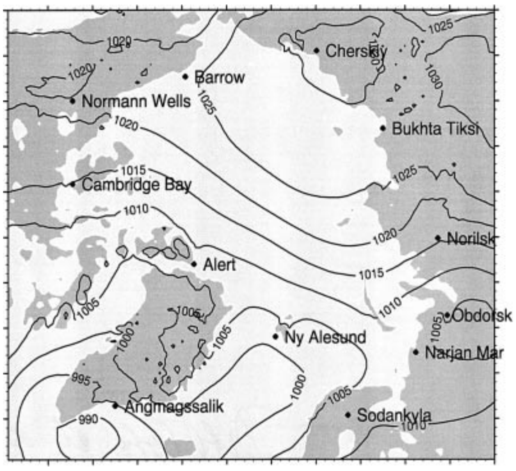

Fig. 11. Monthly mean sea level pressure (hPa) for January 1991 simulated with the ECHAM3_MO scheme and the selected individual stations for comparison of the vertical temperature profiles.

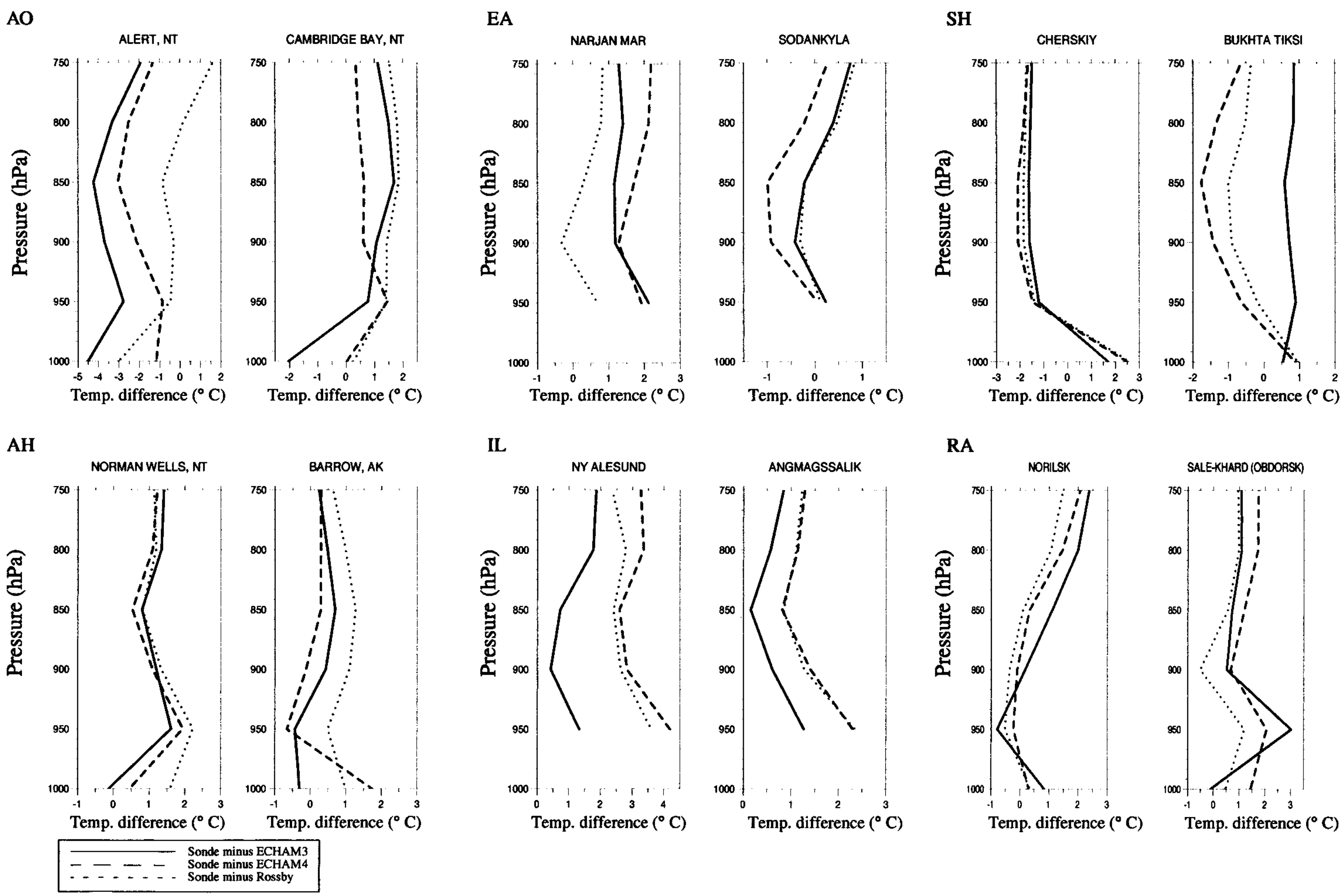

Fig. 12. Monthly mean vertical profiles at individual grid points in the main areas SH, RA, EA, IL, AO, AH for January 1991, showing the air temperature differences (°C) "radiosonde observation data minus simulations". The simulations were performed with the ECHAM3_MO scheme (solid lines), the ECHAM4 version (dashed lines) and the ECHAM3_RO scheme (dotted lines).

observed monthly means were computed on the basis of at least 21 daily values using the Historical Arctic Radiosonde Archive data, HARA (1996). In case of less values no monthly mean was computed, which is the reason for missing data at some stations in Fig. 12. The model simulations were interpolated on the coordinates of the station points. The model simulations are general in good agreement with the radiosonde data. The deviations range from −4.5°C to 3°C. At the stations Chiersky and Bukhta Tiksi (SH) the ECHAM_RO and the ECHAM3_MO schemes produce the best results. At the stations Norilsk and Obdorsk (RA), the profiles are quite similar and the differences are small, nevertheless ECHAM3_RO shows the best agreement. Also at the stations Narjan Mar and Sodankylä (EA) the ECHAM3_RO scheme is the better choice. At the stations Ny Ålesund and Angmagssalik (IL) the ECHAM3_MO scheme clearly simulates the observations best. At the stations Alert and Cambridge Bay (AO) larger differences occur, but ECHAM4 and ECHAM3_RO give the best agreement. At the stations Norman Wells and Barrow (AH) the differences are small and the temperature profiles are simulated better by the ECHAM3_MO scheme.

Table 1 specifies the temperature differences between radiosonde observations and simulations as altitude means between 1000 and 750 hPa for January 1991 at 27 stations distributed over the whole Arctic (Fig. 13). Irrespective of the PBL parameterization scheme used, deviations from the radiosonde data are relatively moderate at most

Table 1. *Monthly mean temperature differences "radiosonde observations minus simulations in °C", height averaged over 750–1000 hPa, January 1991*

Station name	ECHAM3_MO	ECHAM4	ECHAM3_RO
Cherskiy	−0.96	−1.11	−0.99
Mys Shalaurova	1.51	0.25	0.84
Bukhta Tiksi	0.73	−0.82	−0.34
Olenek	−0.70	−1.91	−1.90
Khatanga	1.15	−0.55	−0.82
Norilsk	0.96	0.64	0.35
Obdorsk	1.05	1.48	0.61
Narjan Mar	1.43	1.84	0.46
Ostrov Vize	3.01	3.12	1.55
Krenkelya	4.05	4.36	2.89
Sojna	1.61	1.08	0.70
Murmansk	0.91	0.74	0.75
Sodankylä	−1.38	−1.70	−0.61
Barentsburg	2.65	4.83	4.14
Ny Ålesund	2.34	4.37	3.66
Danmarkshavn	−0.98	1.29	1.43
Angmagssalik	0.69	1.39	1.36
Egedesminde	−1.39	−0.81	−0.43
Alert	−3.41	−1.84	−0.48
Hall Beach	1.24	1.45	1.94
Resolute Bay	0.01	0.07	1.23
Eureka	−4.01	−2.55	−1.51
Mould Bay	−0.21	−0.73	0.72
Cambridge Bay	0.68	0.58	1.38
Norman Wells	1.04	1.06	1.38
Inuvik	0.32	0.49	0.32
Barrow	0.19	0.31	0.91
mean over all stations	0.46	0.64	0.72
standard deviation	1.77	1.91	1.42

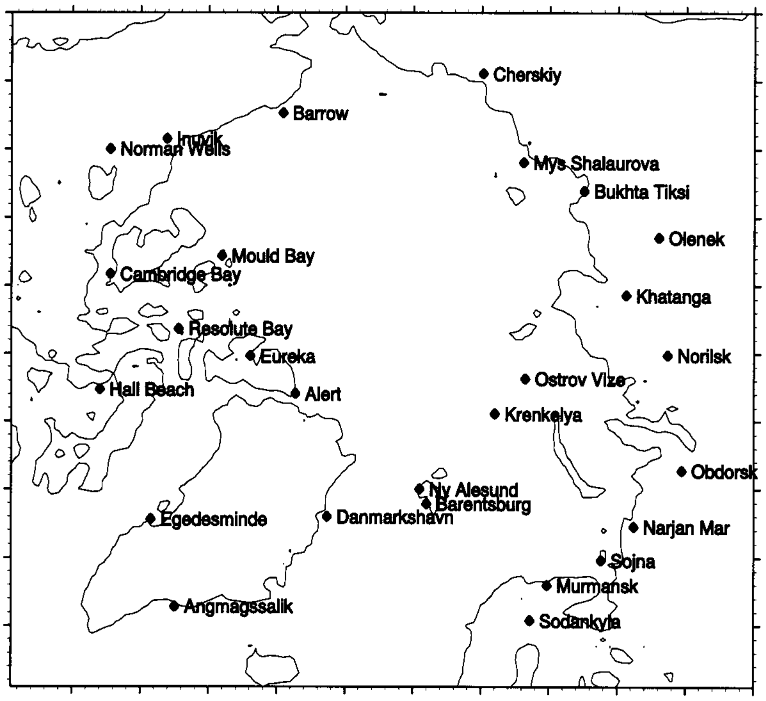

Fig. 13. Geographical distribution of 27 Arctic radiosonde stations chosen for comparison of the results in Table 1.

stations. At the stations Barentsburg, Ny Ålesund, Ostrov Vize, Krenkelya and Eureka the height averaged deviations are in the range between -1.5°C and 4.8°C. The strong deviations between these stations are mainly connected with the unrealistically prescribed constant model sea ice thickness over the Arctic Ocean. At all other stations the height averaged deviations are smaller than 2°C. The mean height averaged deviation of the modeled temperatures from the radiosonde data averaged over all stations are 0.46 ± 1.77°C for ECHAM3_MO, 0.64 ± 1.91°C for ECHAM4 and 0.72 ± 1.42°C for ECHAM3_RO. The error in the radiosonde data itself is in the range of 0.2°C. The ECHAM3_RO scheme simulates the smallest and the ECHAM4 version the largest standard deviation.

For stations mainly located over the Russian and European Arctic, ECHAM3_RO delivers the best agreement (Table 1). For the stations influenced by the Atlantic Ocean the ECHAM3_MO parameterization works better. The Rossby-number similarity scheme simulates more successfully the cold and stable PBL over land surfaces during winter, whereas the ECHAM3_MO version describes better the convective PBL over stations influenced by transport of warmer air from the ocean.

The scope of this paper was not to find the best adapted parameterization, but instead to show the strong influence of fundamentally different parameterization concepts, currently used in climate models of the Arctic. Although it is difficult to compare local station data against model profiles simulated with a horizontal resolution of 50 km by 50 km over areas with pronounced orography and land-sea contrasts which can exert strong local effects on the vertical temperature profiles, the results suggest that the Rossby number similarity is more appropriate for use in Arctic climate models.

4. Summary

A 1-dimensional column model with two different PBL parameterization schemes was developed for monthly integrations in order to study the influence of different parameterization of turbulent exchange processes on the simulated local vertical structure of the atmosphere and the atmosphere–surface energy exchange. The first scheme uses the ECHAM3 boundary layer parameterization, including the Monin–Obukhov similarity theory in the surface layer and a mixing length approach above. The second scheme applies Rossby-number similarity theory for the whole PBL, connecting external parameters with turbulent fluxes and with universal dimensionless functions on the basis of Arctic data. The heat and humidity advection is approximated as residual term of the PBL balance equation, where diabatic sources are determined from the current model solution and local temperature and humidity changes are estimated from radiosonde data.

For January conditions, a significantly stronger stable stratification connected with pronounced negative heat fluxes throughout the planetary boundary layer has been obtained by applification of the Rossby-number similarity theory compared to the results with Monin–Obukhov similarity theory and mixing length approach. In comparison with the Rossby-number similarity, the MO-mixing length parameterization underestimates stable conditions in the Arctic PBL.

In order to investigate the influence of different PBL parameterization schemes on large-scale atmospheric circulation structures monthly integrations of the 3-dimensional regional climate model HIRHAM over the Arctic with a horizontal resolution of 0.5° have been carried out, using ECHAM3 with Monin–Obukhov similarity theory in the surface layer and a mixing length approach above, ECHAM3 with Rossby-number similarity theory and ECHAM4 turbulent kinetic energy closure. The results found in the 1-dimensional January simulations are comparable with the 3-dimensional simulations, where Rossby-number similarity theory produces a more stable stratification over the whole Arctic compared with the ECHAM3 Monin–Obukhov similarity theory in the surface layer and a mixing length approach above. The comparison with radiosonde data of selected Arctic stations for January shows that using ECHAM3 with Rossby-number similarity theory the cold and stable PBL over land surfaces during winter is more successfully simulated. Our results concerning the influence of different PBL schemes on the Arctic climate are in qualitative agreement with those of Giorigi et al. (1993). Their study elaborated over a European integration area, that changes in the PBL and the radiative transfer schemes significantly affected the modelled temperature and cloudiness.

The use of different PBL parameterizations for climate model integrations leads to different energy fluxes from the surface into the atmosphere. These differences are of the same order as those due to surface heat flux variations connected with synoptic-scale changes. Therefore, changes in the Arctic PBL parameterization would result in different baroclinic structures formation. Owing to the high sensitivity of the Arctic climate structures to the applied PBL parameterization different synoptic ensembles can be developed and the climate model generates different Arctic circulation structures. Possible climatic changes in the Arctic surface climate as expected by models would be accompanied by impacts on the cloud cover and the inversion layer, which develops in the stable Arctic PBL. Viterbo et al. (1999) showed that the ECMWF model had the tendency to produce a severe cold bias over continental areas in winter. They showed that the stable boundary scheme alike our ECHAM3 Monin–Obukhov similarity theory in the surface layer and a mixing length approach above has an inherent positive feedback that amplifies a near-surface cold bias. ECHAM3 with Rossby-number similarity theory seems to avoid such cold bias on the surface. The interactions between cold surfaces, frozen soil and permafrost and the stable stratified atmospheric boundary layer remain poorly understood and need further research.

5. Acknowledgements

The HIRLAM system was developed by the HIRLAM project group, a cooperative project of the national weather services in Denmark, Finland, Iceland, Ireland, the Netherlands, Norway, Sweden and Spain. The authors are grateful to E. van Mejjgaard, KNMI de Bilt and J. H. Christensen, DMI Copenhagen, who developed the 1-dimensional version of the regional climate model HIRHAM. We thank Dörthe Handorf, AWI Potsdam for helpful and illuminating discussions and Helga Henschel and

Antje Weisheimer, AWI Potsdam for improving our English. The authors appreciate the very useful comments of two anonymous reviewers, which helped to clarify the presentation and interpretation of the results. V. F. Romanov appreciates the Russian Fundamental Research Foundation for financial support of the PBL parameterization development under Project 98-05-65189.

REFERENCES

Abegg, C. 1999. Parameterization of atmospheric boundary layer processes in a regional climate model of the Arctic. *Reports on Polar Research* **311**, 120 pp (in German).

Betts, A. K. and Miller, M. J. 1986. A new convective adjustment scheme (II) Single column tests using GATE wave, BOMEX, ATEX, and arctic air-mass data sets. *Q. J. R. Meteorol. Soc.* **112**, 693–709.

Blackadar, A. K. 1962. The vertical distribution of wind and turbulent exchange in a neutral atmosphere. *J. Geophys. Res.* **67**, 3095–3102.

Blackadar, A. K. 1967. External parameters of the wind flow in the barotropic boundary layer of the atmosphere. *Proc. GARP Study Conference*, Stokholm, WMO.

Brinkop, S. and Roeckner, E. 1995. Sensitivity of a general circulation model to parameterizations of cloud-turbulence interactions in the atmospheric boundary layer. *Tellus* **47A**, 197–220.

Bromwich, D. H., Tzeng, R. Y. and Parish, T. R. 1994. Simulation of the modern Arctic climate by the NCAR CCM1. *J. Climate* **7**, 1050–1069.

Christensen, J. H. and Van Mejjgaard, E. 1992. On the construction of a regional climate model. *Tech. Rep.* **92-14**. DMI, Copenhagen.

Christensen, J. H., Christensen, O. B., Lopez, P., Van Meijgaard, E. and Botzet, M. 1996. The HIRHAM4 regional atmospheric climate model. *DNMI Sci. Rep.* **96-4**, Dan. Meteorol. Inst., Copenhagen, 51 pp.

Claussen, M., Lohmann, U., Roeckner, E. and Schulzweida, U. 1994. A global data set for land surface parameters. *MPI Rep.* **135**. MPI Hamburg.

Curry, J. A., Rossow, W. B., Randall, D. and Schramm, J. L. 1996. Overview of Arctic cloud and radiation characteristics. *J. Clim.* **9**, 1731–1764.

Cuxart, J., Bougeault, P., Lacarrere, P., Noilhan, J. and Soler, M. R. 1994. A comparison between transilient turbulence theory and the exchange coefficient model approaches. *Boundary-Layer Meteorology*, **67**, 251–276.

Davies, H. C. 1976. A lateral boundary formulation for multilevel prediction models. *Q. J. R. Meteorol. Soc.* **102**, 405–418.

Derbyshire, S. H. 1995. Stable boundary layers: observations, models and variability. Part I: Modelling and measurements. *Boundary-Layer Meteorology* **74**, 19–54.

Debyshire, S. H. 1999. Boundary-layer decoupling over cold surfaces as a physical boundary-instability. *Boundary-Layer Meteorology* **90**, 297–325.

Dethloff, K., Rinke, A., Lehmann, R., Christensen, J. H., Botzet, M. and Machenhauer, B. 1996. Regional climate of the Arctic atmosphere. *J. Geophys. Res.* **101**, 23,401–23,422.

DKRZ, 1992. The ECHAM3 atmospheric general circulation model. *Tech. Rep.* **6**. Modellbetreuungsgruppe, Hamburg, 184 pp.

Dümenil, L. and Todini, E. 1992. A rainfall-runoff scheme for use in the Hamburg climate model. In: J. P. Kane (ed.): *Advances in theoretical hydrology — a tribute to James Dooge*. Elsevier Science Publishers, pp. 129–157.

Giorgetta, M. and Wild, M. 1995. The water vapour continuum and its representation in ECHAM4. *MPI Rep.* **162**, 38 pp., Hamburg.

Giorgi, F., Marinucci, M. R. and Bates, G. T. 1993. Development of a second-generation regional climate model (RegCM2). Part 1: Boundary layer and radiative transfer processes. *Mon. Wea. Rev.* **121**, 2794–2831.

Gustafsson, N. 1993. HIRLAM 2 final report. *HIRLAM Tech. Rep.* **9**, 126 pp., Norrköping.

Handorf, D., Foken, T. and Kottmeier, C. 1999. The stable atmospheric bondary layer over an antarctic ice sheet. *Boundary-Layer Meteorology* **91**, 165–189.

HARA, 1996. National Snow and Ice Data Center (NSIDC). *Historical Arctic Rawinsonde Archive*, vol. **3–5**. CD-ROM, Boulder, Colo.

Hense, A., Kerschgens, M. and Raschke, E. 1982. An economical method for computing radiative transfer in circulation models. *Q. J. R. Meteorol. Soc.* **108**, 231–252.

Jürrens, R. 1999. Validation of surface fluxes in climate simulations of the Arctic with the regional model REMO. *Tellus* **51A**, 698–709.

Kazansky, A. B. and Monin, A. S. 1960. On the turbulent regime above air-surface-layer. *USSR Academy of Science News. Geophys. Ser.* **1**, 165–168.

Louis, J.-F. 1979. A parametric model of vertical eddy fluxes in the atmosphere. *Boundary-Layer Meteorology* **79**, 107–130.

Lynch, A. H., Chapman, W. L., Walsh, J. E. and Weller, G. 1995. Development of a regional climate model of the western Arctic. *J. Climate* **8**, 1555–1570.

Machenhauer, B. 1988. The HIRLAM final report. *HIRLAM Tech. Rep.* **5**, 116 pp. Copenhagen.

McNider, R. T., England, D. E., Friedman, M. J. and Shi, X. 1995. Predictability of the stable atmospheric boundary layer. *J. Atmos. Sci.* **52**, 1602–1614.

Miller, M. J., Palmer, T. N. and Swinbank, R. 1989. Parameterization and influence of sub-grid scale orography in general circulation and numerical weather prediction models. *Meteorol. Atmos. Phys.* **40**, 84–109.

Monin, A. S. and Zilitinkevich, S. S. 1967. Planetary boundary layer and large-scale atmospheric dynamics. *Proc. GARP Study Conference*. Stokholm, WMO.

Monin, A. S. and Yaglom, A. M. 1971. *Statistical fluid mechanics, mechanics of turbulence*. MIT Press, Cambridge, 769 pp.

Morcrette, J.-J. 1989. Description of the radiation scheme in the ECMWF model. *Tech. Memo.* **165**, ECMWF, Reading.

Nordeng, T. E. 1994. Extended versions of the convective parameterization scheme at ECMWF and their impact on the mean and transient activity of the model in the tropics. *Tech. Memo.* **206**, ECMWF, Reading.

Overland, J. E., Adams, J. M. and Bond, N. A. 1997. Regional variations of winter temperatures in the Arctic. *J. Climate* **10**, 821–837.

Overland, J. E. and Guest, P. S. 1991. Control of minimum snow and air temperatures over Arctic sea ice during winter. *J. Geophys. Res.* **96**, 4651–4662.

Palmer, T. N., Shutts, G. J. and Swinbank, R. 1986. Alleviation of a systematic westerly bias in general circulation and numerical weather prediction models through an orographic gravity wave drag parameterization. *Q. J. R. Meteorol. Soc.* **112**, 1001–1039.

Pinto, J. O. and Curry, J. A. 1997. Rôle of radiative transfer in the modeled mesoscale development of summertime arctic stratus, *J. Geophys. Res.* **102**, 13,861–13,872.

Pinto, J. O., Curry, J. A., Lynch, A. H. and Persson, P. O. 1999. Modelling clouds and radiation for the November 1997 period of SHEBA using a column climate model. *J. Geophys. Res.* **104**, 6661–6678.

Randall, D. A., Xu, K.-M., Somerville, R. J. and Iacobellis, S. 1996. Single column models and cloud ensemble models as links between observations and climate models, *J. Climate* **9**, 1683–1697.

Randall, D. et al. 1998. Status and outlook for large-scale modeling of atmosphere–ice–ocean interactions in the Arctic. *Bull Amer. Met. Soc.* **78**, 197–219.

Randall, D. A. and Cripe, D. G. 1999. Alternative methods for specification of observed forcing in single-column models and cloud system models. *J. Geophys. Res.* **104**, 24,527–24,545.

Rinke, A., Dethloff, K., Christensen, J. H., Botzet, M. and Machenhauer, B. 1997. Simulation and validation of Arctic radiation and clouds in a regional climate model. *J. Geophys. Res.* **103**, 29,833–29,847.

Rinke, A., Dethloff, K. and Christensen, J. H. 1999. Arctic winter climate and its interannual variations simulated by a regional climate model. *J. Geophys. Res.* **104**, 19,027–19,038.

Roeckner, E., Rieland, M. and Keup, E. 1991. Modelling of cloud and radiation in the ECHAM4 model. In: ECMWF/WCRP Workshop on Clouds, radiative transfer and the hydrological cycle, 12–15 November 1990, pp. 199–222. ECMWF, Reading.

Roeckner E. et al. 1992. Simulation of the present-day climate with the ECHAM model: impact of model physics and resolution. *MPI Rep.* **93**, Hamburg, 171 pp.

Roeckner E. et al. 1996. The atmospheric general circulation model ECHAM4: model description and simulation of present-day climate. *MPI Rep.* **218**, 90 pp, Hamburg.

Romanov, V. F. 1976a. The parameterization of nonlinear small-scale atmosphere–ice–ocean interactions. *Meteorology and Hydrology* **12**, 49–59.

Romanov, V. F. 1976b. Vertical motions and turbulent regime in the planetary boundary layer. *USSR Academy of Science News. Atmospheric and Oceanic Physics* **12**, 478–484.

Romanov, V. F. 1977. The similarity theory for the baroclinic atmospheric boundary layer. *USSR Academy of Science News. Atmospheric and Oceanic Physics* **13**, 1081–1086.

Romanov, V. F., Ariskina, N. V., Vasilljev, V. F. and Lagun, V. J. 1987. Energetics of the atmosphere in polar regions (in Russian). *Gidrometeoizdat Leningrad*, 296 pp.

Serezze, M., Kahl, J. D. and Schnell, R. C. 1992. Low-level temperature inversions of the Eurasian Arctic and comparisons with Soviet drifting station data. *J. Clim.* **5**, 615–629.

Sundquist, H. 1978. A parameterization scheme for non-covective condensation including prediction of cloud water content. *Q. J. R. Meteorol. Soc.* **104**, 677–690.

Tiedtke, M. 1989. A comprehensive mass flux scheme for cumulus parameterization in large-scale models. *Mon. Wea. Rev.* **117**, 1779–1800.

Tilley, J. S. and Lynch, A. H. 1998. On the applicability of current land surface schemes for Arctic tundra: an intercomparison study. *J. Geophys. Res.* **103**, 29,051–29,063.

Viterbo, P., Beljaars, A., Mahfouf, J. F. and Teixeira, J. 1999. The representation of soil moisture freezing and its impact on the stable boundary layer. *Q. J. R. Meteorol. Soc.* **125**, 2401–2426.

Walsh, J. E., Lynch, A., Chapman, W. and Musgrave, D. 1993. A regional model for the atmosphere–ice–ocean interaction in the western Arctic. *Meteorol. Atmos. Phys.* **51**, 179–194.